Final Report Addendum NAS 9-10484

EXTENDABLE NOZZLES FOR SPACE ENGINES

Report 10484-FRA 30 July 1971

AEROJET LIQUID ROCKET COMPANY
A DIVISION OF AEROJET GENERAL
SACRAMENTO, CALIFORNIA

Final Report Addendum

30 July 1971

Report 10484-FRA

EXTENDABLE NOZZLES FOR SPACE ENGINES

Prepared Under
Contract NAS 9-10484

for

NATIONAL AERONAUTICS AND SPACE ADMINISTRATION
Manned Spacecraft Center
Houston, Texas

AEROJET LIQUID ROCKET COMPANY
Sacramento, California

Report 10484-FRA

TABLE OF CONTENTS

LIST OF TABLES

LIST OF FIGURES

FOREWORD

This report, whose purpose is to present the findings of analysis of the extendable nozzles for space engines test program, is submitted in partial compliance with the requirements of Contract NAS 9-10484.

The contents of this report completes the technical effort and satisfies the program objectives as defined by the contract and is intended to verify and/or upgrade Volume I (Program Studies) and Volume II (Design Guide) of the Final Report (10484-FR).

All work under the subject contract was performed for the National Aeronautics and Space Administration's Manned Spacecraft Center, Houston, Texas, by the Aerojet Liquid Rocket Company. The program was under the direction of Dr. N. E. Van Huff, Program Manager; R. C. Schindler, Project Manager; and E. Schmauderer, Project Engineer. The NASA Project Engineer for the program was Mr. G. Hubbard.

I. INTRODUCTION

The objective of the Extendable Nozzles for Space Engines Program was to prepare a comprehensive design guide for extendable/retractable nozzle extensions for space engine applications.

The program was conducted in two overlapping phases, extending from 12 January 1970 to 30 July 1971. The first phase was devoted to engineering analysis and the design of an experimental thrust chamber incorporating an extendable/retractable nozzle extension. The second phase consisted of fabrication of the Phase I thrust chamber design, continued engineering analysis, and delivery of the thrust chamber to the NASA White Sands Test Facility where it was to be tested. The data derived from the experimental testing was to be used in conjunction with or to upgrade the results of analysis. Delays in testing resulted in preparation of the final report and design guide without benefit of the experimental data derived from testing.

This document presents the findings of analysis of the experimental test data, upgrading the Final Report (10484-FR).

II. SUMMARY

This section serves to summarize the conclusions and recommendations derived from analysis of the experimental extendable/retractable nozzle test data and to evaluate the impact of these results on Volume I (Program Studies) and Volume II (Design Guide) of the final report.

A. SUMMARY OF ANALYTICAL CONCLUSIONS

The conclusions resulting from the test data analysis are as follows:

- Heat flux in the area of gas reattachment downstream of a rearward facing step increased significantly as height of the step was increased. An increase in heat flux of up to 2.5 times that for a smooth wall was measured (Figure 1).

- Nozzle performance, $I_{sp(del)}$, significantly reduced as the height of a rearward-facing step was increased (Figure 2).

- Supplemental supersonic film cooling (GN_2) of the hot gas reattachment zone on the nozzle wall downstream of a rearward facing step was highly effective. A minimum amount of film coolant was required to reduce the uncooled heat loads (Figures 3, 4 and 5).

- Of the two nozzle sealing concepts tested, the static face seal (as recommended in the final report) is the most desireable for incorporation into an extendable/retractable nozzle design.

- Nozzle deployment and retraction, with the engine firing, was successfully demonstrated under simulated altitude conditions.

II, Summary and Comparison of Conclusions (cont.)

B. IMPACT OF ANALYSIS ON FINAL REPORT

1. Heat Transfer

At the point of gas reattachment in the step region of the extendable nozzle, the design guide recommended that the maximum heat flux be calculated using Newton's law of cooling and an amplified heat transfer coefficient. The heat flux would therefore be calculated as

$$q = h(T_{wa} - T_w)$$

where q = heat flux
h = step region film coefficient
T_{wa} = adiabatic wall temperature
T_w = nozzle wall temperature

An amplification factor of 3.0 was recommended, so that the step region film coefficient equation became:

$$h = 3.0\ hg$$

where 3.0 = recommended amplification factor
$*h_g$ = smooth wall film coefficient

The step region coefficient, h, was not determined experimentally during the extendable nozzle test program since the calorimeters needed to supply data used in calculating this parameter did not operate properly. However, using the 3.0 amplification ratio, it can be stated

$$\frac{q}{q_o} = 3.0$$

*Normally calculated for rocket nozzles using Bartz equation or an equivalent correlation.

II, B, Impact of Analysis on Final Report (cont.)

where q = step region heat flux

q_o = smooth wall heat flux

Accordingly, a heat flux ratio of film cooled to smooth wall flux might also be used for design. The experimentally determined nozzle heat flux data showed that the maximum step region heat flux depended on step size, and the amplification factor varied between 1.0 and 2.5.

$$\frac{q}{q_o} = 1.0 \text{ to } 2.5^*$$

Therefore, it is concluded from these data that an amplification factor of 3.0 applied to either the smooth wall film coefficient or the smooth wall heat flux will give a conservative estimate of step region heat transfer.

With film cooling, Newton's law of cooling was also recommended with an amplification factor of 3.0 applied to the film coefficient as before. The adiabatic wall temperature with film cooling is caluclated using Goldstein's correlation:

$$\eta = \frac{T_{wa}-T_c}{T_r-T_c} = 1.0, \ \xi \leq 15.5$$

$$\eta = \left(\frac{15.5}{\xi}\right)^{2.5}, \ 15.5 < \xi < 39.0$$

*Based on experimental smooth wall data.

II, B, Impact of Analysis on Final Report (cont.)

where $\xi = \left(\frac{x}{h}\right)\left(\frac{T_o}{T_c}\right)\left(\frac{1}{M}\right)^{0.27}$

x = film cooled length

h = coolant slot height

T_o = mainstream gas stagnation temperature

T_c = coolant supply temperature

M = ratio of coolant to mainstream mass velocity

T_{wa} = adiabatic wall temperature

T_r = free stream recovery temperature

Series III, Test-003 data are compared to this prediction in the step region and downstream of the step in Figure 7. The predicted heat flux was calculated with the recommended amplification factors of 3.0 and 1.0, and these curves are shown in the figure. Comparison of the data to these predictions shows that the 3.0 amplification factor is overly conservative in the step region where a 1.0 factor appears to be adequate. Also, downstream of the step, the prediction with a 1.0 amplification factor is seen to provide a conservative estimate of the film-cooled wall heat flux.

2. Performance

The Design Guide recommendation, that a deployable nozzle should be designed for a minimum of discontinuity at the interface between the fixed portion of the nozzle and the movable extension to minimize the loss in performance ($I_{sp(del)}$) resulting from discontinuities in the nozzle wall, was verified during this study. The experimental data, Figure 2, shows that the loss in nozzle performance versus step height (wall discontinuity) increases with step height.

At the time the Final Report was prepared, neither analytical nor experimental data was available for predicting the magnitude of nozzle losses resulting from discontinuities; these losses were assumed to be small for properly designed joints, i.e., joints with minimum discontinuity.

II, B, Impact of Analysis on Final Report (cont.)

Consequently, the performance data presented in the final report does not include losses attributable to nozzle wall discontinuities.

The delivered performance ($I_{sp(del)}$) for each nozzle configuration presented in the Design Guide was estimated by calculating the one-dimensional kinetic vacuum specific impulse and subtracting the various real engine losses using the following equation:

$$I_{sp(del)} = I_{sp(odk)} - I_{sp(er/mrd)} - \Delta I_{sp(bl)} - \Delta I_{sp(div)} - \Delta I_{sp(c)}$$

where
- $I_{wp(odk)}$ = one-dimensional kinetic vacuum specific impulse based on injector mixture ratio
- $\Delta I_{sp(er/mrd)}$ = specific impulse loss due to energy release and mixture ratio maldistribution
- $\Delta I_{sp(bl)}$ = specific impulse loss due to boundary layer effects
- $\Delta I_{sp(div)}$ = specific impulse loss due to flow divergence at the nozzle exit
- $\Delta I_{sp(c)}$ = specific impulse loss due to nozzle extension cooling

The use of this equation is restrictive and should be expanded to include an estimate of the nozzle performance losses associated with nozzle wall discontinuities. Unfortunately, the loss in $I_{sp(del)}$ as presented in Figure 2, is indicative of the uncooled nozzle losses experienced with the experimental test engine only. Close inspection of the uncooled nozzle performance data does indicate that even small nozzle wall discontinuities produce performance losses and that the engine designer should not assume these losses equal to zero, no matter how small the wall discontinuity. Care should be taken by the designer when attempting to predict losses associated with small nozzle wall discontinuities, for it is conceivable that, as the attachment area ratio becomes smaller, the performance loss increases for a given wall discontinuity. That is to say, that the C_f for a given nozzle configuration is a larger function of the smaller area ratios and not so much the larger

II, B, Impact of Analysis on Final Report (cont.)

area ratios, and that a wall discontinuity at a small area ratio would produce a larger performance loss than the same discontinuity at a larger area ratio. Therefore, a nozzle performance loss for discontinuities up to 0.25 in. could reach 2.0 lb-sec/lb or more. Another factor to consider is that the performance loss presented in Figure 2 is associated with the configuration of the discontinuity tested and, for a discontinuity of a different configuration -- even at the same area ratio -- the magnitude of performance loss could be greater or less.

3. Nozzle Sealing and Supplemental Cooling

Evaluation of the data derived from the test program did not yield additional design data to upgrade that presented in the final report. The suggested design techniques, as presented in the final report, remain valid.

4. Nozzle Deployment and Retraction

No data adversely affecting the design recommendations established and presented in the final report were developed during evaluation of the nozzle deployment and retraction system. The recommended design approach and considerations, as presented in the final report, remain valid.

III. TEST PROGRAM

A. OBJECTIVE

The objectives of the experimental extendable nozzle test program were (1) to evaluate the effect of contour mismatch at the nozzle attachment interface on heat transfer and performance, (2) to evaluate the feasibility of film cooling at the nozzle attachment interface, (3) to evaluate sealing of the interface between the fixed and movable portions of the nozzle, and (4) to demonstrate the operation of an extendable - retractable nozzle extension with the engine firing under simulated altitude conditions.

B. DESCRIPTION OF TEST HARDWARE

To satisfy the test program objectives, the test engine was configured to permit evaluation of : (1) a change in step heights; (2) the addition of auxiliary film cooling of the nozzle extension downstream of the divergent step, as well as various sealing concepts; and (3) nozzle deployment and retraction. The test engine shown in Figure 6 was designed around the NASA-supplied LEM workhorse injector and chamber. This limited the quantity of new components to those areas which were related to the extendable nozzle. The new designs consisted of a chamber - nozzle adapter, a nozzle film coolant injector, nozzle deployment and retraction system, and a nozzle extension.

1. Nozzle Extension

The nozzle extension (heat-sink design) was made of 347 stainless steel with a constant wall thickness of 0.200 in. It had a cylindrical section several inches long so as to put the attachment flange in a cooler area and provide interfaces to accept the several different sealing concepts to be evaluated. Nine calorimeters, 24 thermocouples, and 14 pressure taps

III, B, Description of Test Hardware (cont.)

were used to monitor thermal and pressure conditions throughout the extension. A Rao contour was selected for the entire nozzle assembly and the rigid, heat-sink extension duplicates this contour from an area ratio of approximately 22:1 out to 37.1.

Instrumentation was concentrated in the predicted hot gas reattachment locations on the nozzle wall for the different fixed-nozzle step conditions to be evaluated (Figures 8 and 9).

2. Chamber-Nozzle Adapter

The chamber - nozzle adapter was designed to physically bridge the area from the LEM chamber to the movable nozzle extension. The adapter served as the backbone of the design, supporting all other components and serving as interface between the entire assembly and a thrust takeout or measuring system provided by the test facility. Further, it provided the capability of delivering a secondary cooling flow to the reattachment area and the inner wall of the nozzle extension for evaluation of this cooling technique. It also supported the nozzle guide and actuation systems required to translate the nozzle, and served as a support for the seals necessary to seal the moving and fixed portions. Finally, it provided a variable geometry at the end of the fixed portion of the tip in order to determine the effect of different fixed-to-movable transition step heights or configurations (Figures 6 and 10).

3. Film Coolant Injector

The supersonic injector used for injecting nitrogen into the reattachment area was an integral part of the nozzle-chamber adapter. The injector not only provided evenly distributed coolant by 180 two-dimensional nozzles but incorporated removable tips (as shown in Figure 11) to provide

III, B, Description of Test Hardware (cont.)

discontinuities in the nozzle wall of zero in., 0.25 in., 0.50 in., and 0.75 in. for testing in both cooled and uncooled states. The coolant injector provided coolant mass flow control from zero lb/sec to 0.5 lb/sec to the step region. The coolant injector velocities ranged from 1291 ft/sec at 0.1 lb/sec flow to 1485 ft/sec at 0.5 lb/sec.

4. Nozzle Deployment and Retraction System

Three separate items made up the nozzle deployment and retraction system. They were the actuation system, the guide and support system, and the nozzle slide section (Figure 6).

a. Nozzle Actuation System

The nozzle actuation system was composed of three single-rod hydraulic actuators. The actuators connected directly the movable nozzle to the engine frame and distributed loads equally about the three rails used in the guide system. Actuation speed was controlled by matched orifices in the hydraulic supply and discharge lines.

b. Guide and Support System

The guide and support system functioned as the name implies -- support the moving hardware (in this case, the slide section and exit cone attached to it) at all times under all loads, whether extended or retracted, and guide it so as to achieve proper radial clearances and alignment when deployed.

The guide/support system selected for use was the Thomson Industries' ball bushing system. The rails or guides consisted of case hardened centerless ground steel rods which were mounted to the three

III, B, Description of Test Hardware (cont.)

support gussets of the chamber-nozzle adapter by bolts and spacers, allowing shims to be added for final adjustment of nozzle alignment. The ball bushing was open, permitting the rail stands to pass through the longitudinal slot in the bushing.

The bushing is a housing which supports rows of longitudinally recirculating ball bearings which roll between the shaft and the housing, contacting the shaft around 75 to 80% of its circumferential surface. The housing (bushing) was, in turn, held and clamped in the hardware to be moved (slide section and extension).

c. Slide Section

The nozzle slide section (as shown in Figure 6) served four distinct functions:

(1) It held the bushings which ride the guide rails and supported them.

(2) It served as a fixture to which the nozzle extension was mounted and sealed.

(3) It served as the movable sealing surface for the fixed-to-moving nozzle seals.

(4) It was the point of attachment for the actuation system.

This ring was designed to transmit all transverse loads on the extension to the guides (six roller bushings) and all longitudinal loads to the actuation system.

III, B, Description of Test Hardware (cont.)

5. Fixed-to-Movable Nozzle Seals

Two different sealing concepts were incorporated into the test engine design for evaluation during the test program. They were the concept of face sealing (static) and piston-type (dynamic and/or static) or diametral sealing.

The face seal (as shown in Figure 6) was installed at the interface between the nozzle slide section and the chamber - nozzle adapter. The small flange on the ID of the slide section served as the sealing surface for the conventional O-ring mounted in the forward-looking face of the nozzle adapter.

The piston-type or diametral seal was also located at the interface between the nozzle slide section and the chamber-nozzle adapter. The adapter again provided the O-ring groove on its OD of the fixed part and the ID of the slide section served as the seals mating sealing surface. The elastomeric seal satisfying the requirements for a diametral seal, that the seal requires a minimum force to compress, will seal large radial clearances between mating pars, and will not tend to roll out during relative part movement was the O-ring elastomeric seal (Figure 12). The seal was glued into the O-ring groove on the fixed part to prevent roll-out and was hollow to minimize compression forces required for good sealing.

Both seals, the face and diametral, were made of silicone rubber for use in a high operating temperature environment.

C. EXPERIMENTAL TESTING

The test program, conducted at the NASA/WSTF in Las Cruces, New Mexico, was initiated on 19 February 1971 and concluded on 14 April 1971. During this period, a total of 25 engine tests were conducted at simulated altitude conditions using N_2O_4 and AeroZINE 50 propellants at a nominal mixture

ratio of 1.6 and chamber pressure of 100 psia. Photographs of the test engine mounted in the testing facility are shown in Figures 13, 14, and 15. Seven of these tests were classified as system balance and data point verification tests, while the remaining 18 tests satisfied the program objectives. The test data for the 18 tests are summarized in Table I. A summary of the 25 engine fire test is enclosed as Table II. The detailed test plan was included as Appendix B of the final report for this program, Extendable Nozzles for Space Engines, Volume I, Report No. 10484-FR.

The test program was divided into five discrete test series, each satisfying specific predefined test objectives. The test series and objectives are also shown in Table I.

Test Series No. I established the base performance of the test engine with a continuous divergent uncooled nozzle wall. This series consisted of two tests: a base data point and a verification data point.

Test Series II, III and IV were designed to evaluate nozzle wall discontinuities of 0.25 in., 0.50 in., and 0.75 in. at the interface between the extendable and fixed nozzle (shown in Figure 10) and consisted of four tests each. Three of the four tests evaluated the specific wall discontinuity, step height, at coolant flow rates of 0.1 lb/sec, 0.3 lb/sec and 0.5 lb/sec. The fourth test provided an uncooled base performance data point at that step height.

Test Series No. V investigated and demonstrated operation of the test engine with a partially deployed nozzle and deployment and retraction of the nozzle extension with the engine firing. Test Numbers V-001, V-002 and V-003 were the partially retracted tests, and Test No. V-004A was the deployment and retraction test.

III, Test Program (cont.)

D. TEST DATA ANALYSIS

1. Heat Transfer

The experimental test engine employed thermocouples, calorimeters, and gas probes (Figure 9) to obtain thermal data during the test program. The thermal instrumentation was designed to provide data which could be used to calculate the nozzle wall heat flux and the hot gas and GN_2 coolant film temperatures. Twenty-four thermocouples, nine calorimeters, and four gas probes were used to obtain the nozzle test data. The thermal instrumentation locations are summarized in Table III.

The calorimeters were designed to provide equilibrium nozzle wall temperature data that could be readily converted to nozzle wall heat flux. However, the data derived from testing indicated that the calorimeter did not operate properly. The instrument operated in a fashion similar to that of a thermocouple. It was concluded that the insulation between the calorimeter element and the main body was not adequate to prevent the transfer of heat to the body, resulting in the calorimeter responding in a fashion similar to a thermocouple. Therefore, these data were considered invalid and were not included in the thermal analysis. The gas probe temperature data were much lower than expected and were also considered to be in error and omitted from the analysis.

The test nozzle, as stated in Section III,B, was designed to provide nozzle wall discontinuity or step height at the nozzle extension attachment point and thermal test data for discontinuities of 0.25 in., 0.50 in. and 0.75 in. GN_2 film coolant was employed as an auxiliary coolant, and thermal data were obtained with 0.0, 0.1, 0.3 and 0.5 lb/sec film coolant flow. The test data for thirteen tests (indicated by asterisk in Table I) were analyzed.

III, D, Test Data Analysis (cont.)

The thermocouple temperature data were plotted for each test and smooth curves drawn to show the trend of temperature with axial distance. A typical plot for all series III tests (the 0.5-in. step height test case) is shown on Figure 16.

Selected data points were then taken from the temperature curves and utilized in calculating the nozzle wall heat flux. The method of heat flux calculation, which was developed at ALRC and uses the SINDA program, forces the wall surface temperature to follow the thermocouple transient data while calculating the heat flow through an arbitrarily large gas-side conductance. The calculated nozzle wall heat flux is plotted as a function of axial distance on Figures 3, 4 and 5, in which the step region heat flux is compared to both the smooth wall data and the Bartz predicted heat flux. Inspection of the plotted data, temperature and heat flux vs axial distance indicates the following:

- The smooth contour, zero step test (Test No. I-002) showed that the wall heat flux continually decreased with axial distance as was expected.

- The introduction of a step discontinuity in the contour produced a low heat flux region near the step base and a high-heat flux region near the shoulder and showed that this peak heat flux is highly dependent on the step height. The maximum calculated experimental heat flux (0.5 Btu/in.^{2}-sec) was experienced during test with the .75-in. step configuration. The experimental flux of 0.5 Btu/in.^{2}-sec is approximately 2.5 times the experimental smooth wall flux and is twice the heat flux predicted using the Bartz equation.

- The smooth wall data shown on Figures 3, 4 and 5 are 20 to 30% lower than the Bartz prediction. This

III, D, Test Data Analysis (cont.)

deviation of experimental to predicted heat flux was found to be normal and further verified the validity of the test data. Radiation-cooled nozzle temperature data from Apollo and Transtage testing indicate a heat flux approximately 30% lower than the Bartz predicted flux in the nozzle region (Figure 17).

- Relatively small film cooling flows were effective in cooling the step region. The 0.75-in. step data plotted on Figure 5 indicates that 0.1 lb/sec GN_2 was sufficient to alleviate the high local heating rates encountered without film cooling. The GN_2 coolant flow of 0.1 lb/sec represents 1% of the nozzle mainstream gas flow. This is considered a small amount of coolant, particularly since GN_2 is considered a poor coolant by comparison to propellants. Figures 3 through 5 also show that the nozzle wall heating rates downstream of a step region are reduced as film coolant flows are increased. It should be noted that the peak heat flux in the step region is due to impingement of the hot gas which expands from the lip of the step and produces a very localized heat flux spike and that impingement of the hot gas on the film-cooled boundary layer did not completely destroy the effectiveness of the coolant but that the coolant continued to cool the nozzle wall downstream of the hot gas impingement point.

2. Performance

In a retractable - extendable nozzle there will be a small discontinuity between the movable extension and the fixed nozzle. The objective of the performance analysis was to identify the performance loss associated

III, D, Test Data Analysis (cont.)

with the nozzle discontinuities of 0.25 in., 0.50 in., and 0.75 in., as designed into the test hardware.

The nozzle performance (I_{sp}) was calculated and is presented in Table I. A plot of specific impulse vs. step height for both the uncooled and film cooled tests is presented as Figure 2. This data plot shows that a significant loss in performance was experienced. Also, that as the step height was increased, so did the loss in performance (I_{sp}) (up to 3 sec of impulse for a step height of 0.75 in. uncooled).

3. Nozzle Sealing

Sealing of the interface between the fixed and movable nozzle extension was demonstrated on all tests. The concept of a static face seal employing a conventional O-ring satisfactorily sealed the fixed and movable nozzle interface throughout Test Series I through IV and Test V-004A. The same face seal as installed to initiate the test program was still in reuseable condition following 25 tests at the completion of the program. The static diametral sealing concept was satisfactorily demonstrated on Tests V-001, V-002, and V-003. No leakage was observed during any of the tests. Post fire visual inspection of the seals and mating surfaces showed no damage resulting from heat exposure. The face seal O-ring was exposed to a hot gas environment for an accumulated testing duration of approximately 548 seconds. The static diametral seal exposure time was an accumulated 90 seconds.

The piston or diametral sealing technique for dynamic sealing of the interface between the fixed and movable sections of the nozzle extension proved to be unsatisfactory; however, this technique did provide good sealing when used as a static seal.

III, D, Test Data Analysis (cont.)

Buildup of the test engine included installation of the diametrial piston seal. Following a minimum number of nozzle actuations, during which the actuation system appeared to be marginal with respect to deployment and retraction resulting from the increased seal loads required for sealing, the seal was destroyed. Evaluation of the seal following cyclic operation of the nozzle extension indicated the following:

- The technique of glueing the seal into its gland proved satisfactory. The seal remained in its groove and was not rolled out during cyclic nozzle operation.

- A circumferential section on the OD of the seal, seal contact surface with the nozzle slide section, was torn out. This torn section was approximately 3 inches in length. It was concluded that even though the seal was hollow to minimize the compression forces required for good sealing, that the compression forces under dynamic conditions were great enough to cause seal failure. Not only did the seal fail, but the compression forces required for good sealing were sufficiently high enough to restrict cyclic operation of the nozzle extension (nozzle extension and retraction).

The conclusions drawn from a comparative view point of the test results of the two sealing concepts, remain as originally outlined in the final report.

4. Nozzle Deployment and Retraction

Demonstration of the nozzle deployment and retraction system was successfully accomplished by test during Test Series V.

III, D, Test Data Analysis (cont.)

Test No. V-004, originally slated to demonstrate the nozzle deployment and retraction system, was manually terminated after 16 sec of steady-state chamber pressure operation. The nozzle failed to return to its fully extended position during its re-extended cycle. The test sequence of events was as follows:

- Engine start
- At engine start + 5 sec, the nozzle translation system was signalled to retract the nozzle extension.
- The nozzle deployment and retraction system retracted the nozzle extension.
- At engine start + 10 sec, the nozzle translation system was signalled to extend the nozzle extension.
- The nozzle deployment and retraction system extended the nozzle but at a decreasing rate of travel until the ozzle, as viewed on the TV monitor, appeared to have stopped moving halfway through its re-extend cycle.
- The test was manually terminated at FS_1 + 17 sec

It was concluded following a detailed review of the test records and inspection of the test hardware that (1) the test hardware was in refireable condition (without damage); (2) that the hydraulic actuation pressure be increased to the actuators for the repeat test, if the test was to be repeated; (3) that partial demonstration of the nozzle deployment system did not totally demonstrate the system's capability; and (4) that the test should be repeated if possible.

The requirement of increased hydraulic actuation pressure to solve the deployment problem of the nozzle extension was proposed as a result of the identification of the following potential problem areas:

(1) That minor misalignment, resulting from nozzle pressure loads, of the nozzle slide section to the guide rails could result in increased friction and resistance to nozzle travel, which could only be encountered with the engine firing.

III, D, Test Data Analysis (cont.)

(2) That the bundle of instrumentation cabling attached to the movable nozzle (Figure 15) added sufficient additional resistance to prevent nozzle travel.

(3) That the nozzle wall pressure deviations, as observed on Tests V-001 and V-002, from the predicted wall pressure profile contributed to prevent complete deployment of the nozzle extension (Figures 20, 21 and 22).

(4) That all the above contributed in part to prevent fully deploying the nozzle extension.

Functional testing of the hydraulic actuation system revealed that several solenoid-piloted valves would not operate after being electrically powered for over five minutes, probably due to heating. The test procedure called for these valves to be electrically powered for approximately five minutes prior to test. The operational test procedure was modified to prevent unnecessary power application, and the hydraulic system functionally verified to be capable of reliable nozzle extension deployment and retraction.

Test No. V-004A was conducted using the increased hydraulic actuation pressure. The nozzle deployment system performed satisfactorily. The test sequence of events was as follows:

- Nozzle film coolant on ($\dot{w}$ = 0.5 lb/sec)
- Engine start with the nozzle fully extended
- At engine start + 5 sec, the nozzle deployment system was signalled to retract the nozzle extension
- The nozzle extension was retracted in $\approx$ 2.25 sec
- At engine start + 11 sec, the nozzle deployment system was signalled to extend the nozzle extension

III, D, Test Data Analysis (cont.)

- The nozzle was extended in ≈1.1 sec
- At engine start + 15 sec, the nozzle film coolant was turned off
- At engine start + 25 sec, the nozzle deployment system was signalled to retract the nozzle extension
- The nozzle was retracted in ≈2.25 sec
- At engine start + 31 sec, the nozzle deployment system was signalled to extend the nozzle extension
- The nozzle was extended in 1.1 sec
- The test was terminated after 37 sec of steady-state chamber pressure operation

Not only had this test (Test No. V-004A) served to demonstrate operation of the nozzle deployment and retraction system, but it also demonstrated the capability of the static face seal to reseal the movable-to-fixed nozzle interface following the cyclic operation of the nozzle extension.

The nozzle performance data (I_{sp}) is presented in the performance summary, Table I, for Tests V-004 and V-004A. Specific impulse was calculated for both the film-cooled and uncooled portions of the tests and is presented for comparison in the table. The nozzle wall pressure data gathered during the nozzle retract and extend film-cooled cycle was used to calculate nozzle load. This calculated load was plotted vs. nozzle position. The plots are presented as Figures 18 and 19. These plots were made in an attempt to gain insight into the observed deviation in nozzle wall pressures from predicted as recorded on Tests V-001 and V-002 and its effect on nozzle load vs. position. It should be noted that the investigation of this pressure deviation was conducted in support of Test V-004 and V-004A and carried no further than as reported in this document.

The nozzle wall pressure deviations as measured (Figures 20, 21 and 22), were observed to increase to approximately 7 times that predicted (predicted ≈0.84 psia).

III, D, Test Data Anlysis (cont.)

Tests V-001, V-002, and V-003 were configured primarily to evaluate the piston seal and a secondary nozzle wall configuration different than that evaluated during Test Series IV. A comparison of the two 0.75 in. configurations is presented in Figure 23. To evaluate Configuration No. 2 0.75 in. wall discontinuity, thenozzle extension was fixed in a partially retracted position (retracted 2") and the engine fired. The plotted performance data, Figure 24, indicates an increased loss in nozzle performance over that experienced with Configuration No. 1 0.75 in. step height.

IV. SUGGESTED ADDITIONAL EFFORT

It is suggested that additional technical effort, supported by a subscale laboratory test program, be initiated to provide nozzle performance and thermal design data to supplement that obtained from the extendable/retractable nozzle test program and bridge the design gap as identified. This effort would coincide with and support significantly the NASA Space-Oriented Shuttle Program.

The objective of the extendable nozzles for space engines application program, was to provide design data which are applicable to space engines for which it is desired to upgrade performance by incorporating a high expansion ratio nozzle into a system restricted by vehicle or packaging requirements.

The data analysis phase of the experimental nozzle test program provided meaningful extendable/retractable nozzle design information, but it also identified additional areas of special concern to the performance analyst and engine designer. The main area of concern being the observed performance ($I_{sp(del)}$) loss associated with a nozzle wall discontinuity.

The performance analysis phase of this program (final report presentation) established that there is a definite advantage to incorporating an extendable nozzle into an engine system. This analysis considered performance losses resulting from wall discontinuities equal to zero. It is conceivable that with respect to the performance and payload gained by an extendable nozzle, which could be quite small when the performance loss associated with a given wall discontinuity is considered, that it is not economically feasible or worth the small gain in performance to encorporate an extendable nozzle into the engine system. This is particularly true when the effects of changing nozzle attachment area ratio and the configuration of the nozzle wall discontinuity on performance has not been firmly established or understood.

An attempt was made during analysis of the test data to correlate the effect of discontinuity and discontinuity location in the nozzle on nozzle performance loss.

IV, Suggested Additional Effort (cont.)

The conclusions drawn, mainly due to the limited experimental data available were (1) that the nozzle performance loss as measured could only be associated with the configuration tested, and (2) that yes, there is a loss in nozzle performance associated with a nozzle wall discontinuity, and that this loss increases with increasing step height of the discontinuity and possibly with a change in configuration of the nozzle wall discontinuity.

The proposed experimental laboratory program would not only provide an understanding of the performance loss problem, but would provide analytical data to satisfactorily evaluate the areas of design concern identified during evaluation of the test data. The three major areas of design concern are as follows: (1) how is nozzle performance effected by change in discontinuity, both axial and configuration; (2) how are nozzle heat loads effected by change in discontinuity, both axial and configuration; and (3) how effective is supersonic film cooling of the nozzle extension under these new conditions.

The experimental subscale laboratory test program would not only be configured to provide analytical data to effectively evaluate and satisfactorily answer the above areas of concern, but would also investigate the effects of nozzle wall pressure deviations as identified during Tests V-001 and V-002.

TABLE I

TEST DATA SUMMARY

Test Series	Test No.	Test Date	$\dot{w}_f$ lb/sec	$\dot{w}_o$ lb/sec	$\dot{w}_T$ lb/sec	MR	P_c psia	$\dot{w}_{fc}$ lb/sec	F lb	A_t in.^{2}	Data Time sec	Test Dur sec	$\dot{w}_T = \dot{w}_o+\dot{w}_f+\dot{w}_{fc}$ lb/sec	I_{sp} sec	Step Height in.	Effective Step Height in.	Nozzle Position	Series Objectives
I	002	3-3-71	3.995	6.713	10.708	1.680	100.5	0	3200	19.155	9-10	20	10.708	298.8	0	0	Fully extended	Nozzle performance data with continuous wall uncooled
	*002A	3-4-71	4.035	6.902	10.937	1.711	101.7	0	3257	19.150	18-19	20	10.937	297.8	0	0	Fully extended	Nozzle thermal and pressure data Evaluation of static face seal
II	*001	2-19-71	4.023	6.775	10.798	1.684	100.5	0	3207	19.160	13-14	15	10.798	297.0	0.25	0.25	Fully extended	Nozzle performance data both cooled and uncooled with 0.25-in. step height
	*002A	2-19-71	4.037	6.805	10.842	1.685	100.8	0.107	3226	19.165	11-12	15	10.949	294.7	0.25	0.25	Fully extended	Nozzle thermal and pressure data
	*003	2-19-71	4.072	6.789	10.861	1.667	100.5	0.2526	3242	19.172	10-11	15	11.114	291.8	0.25	0.25	Fully extended	Evaluation of static face seal
	*004C	2-19-71	4.092	6.794	10.886	1.660	100.5	0.5259	3264	19.175	6-7	15	11.412	285.9	0.25	0.25	Fully extended	
III	*001	3-9-71	4.090	6.687	10.777	1.635	100.5	0	3193	19.120	9-10	30	10.777	296.3	0.50	0.50	Fully extended	Nozzle performance data both cooled and uncooled with 0.50 in. step height
	*002	3-9-71	4.107	6.645	10.752	1.618	100.5	0.0986	3195	19.127	8-9	30	10.851	294.4	0.50	0.50	Fully extended	Nozzle thermal and pressure data
	*003	3-9-71	4.106	6.627	10.733	1.614	100.5	0.3178	3204	19.135	8-9	30	11.051	289.9	0.50	0.50	Fully extended	Evaluation of static face seal
	*004	3-9-71	4.027	6.961	10.988	1.728	102.4	0.4888	3285	19.144	14-15	30	11.477	286.2	0.50	0.50	Fully extended	
IV	*001	3-25-71	4.022	6.817	10.839	1.694	100.4	0	3204	19.090	14-15	30	10.839	295.6	0.75	0.75	Fully extended	Nozzle performance data both cooled and uncooled with Configuration No. 1 0.75-in. step height
	*002	3-25-71	4.056	6.759	10.815	1.666	100.4	0.0999	3208	19.097	9-10	30	10.915	293.9	0.75	0.75	Fully extended	
	*003	3-25-71	4.066	6.750	10.816	1.660	100.6	0.2947	3220	19.105	8-9	30	11.111	289.8	0.75	0.75	Fully extended	Nozzle thermal and pressure data Evaluation of static face seal
	*004	3-25-71	4.049	6.777	10.826	1.673	100.6	0.4993	3235	19.113	9-10	30	11.325	285.6	0.75	0.75	Fully extended	
V	001	4-2-71	4.018	6.855	10.873	1.706	100.4	0.5024	3223	19.082	14-15	30	11.375	283.3	0.50	0.75	Retracted 2 in.	Nozzle performance data uncooled and film cooled
	002	4-2-71	4.044	6.831	10.875	1.689	100.4	0.1044	3194	19.074	12-13	30	10.979	290.9	0.50	0.75	Retracted 2 in.	Evaluation of Configuration No. 2 step height = 0.75 in.
	003	4-2-71	4.009	6.938	10.947	1.731	100.7	0	3200	19.067	17-18	30	10.947	292.3	0.50	0.75	Retracted 2 in.	Nozzle partially retracted 2 in.
	004	4-6-71	4.08	6.86	10.94	1.681	102.1	.486	3281	19.06	4-5	17	11.43	286.8	0.50	0.50	Fully extended	Nozzle thermal and pressure data
			4.06	6.87	10.93	1.693	101.7	.491	3099	19.06	6-7	17	11.42	271.0	0.50	0.50	Fully retracted	Demonstration of nozzle deployment and retraction with engine firing
	004A	4-14-71	4.045	6.864	10.909	1.697	101.7	0.5032	3266	19.055	4-5	38	11.412	286.2	0.50	0.50	Fully extended	Evaluation of the diametrial static seal on the partially retracted tests
			3.989	6.909	10.898	1.732	101.0	0.5027	3081	19.055	10-11	38	11.401	270.3			Fully retracted	
			3.969	6.926	10.895	1.745	100.6	0.5045	3244	19.055	14-15	38	11.399	284.6	0.50	0.50	Fully extended	Evaluation of the static face seal during demonstration of nozzle deployment and retraction
			3.919	6.957	10.886	1.778	100.3	0	3188	19.055	24-25	38	10.886	292.8	0.50	0.50	Fully extended	
			3.899	6.991	10.890	1.793	100.3	0	3037	19.055	30-31	38	10.890	278.9			Fully retracted	
			3.876	6.999	10.875	1.806	100.3	0	3180	19.055	36-37	38	10.875	292.4	0.50	0.50	Fully extended	

TABLE II

EXTENDABLE NOZZLE ENGINE TEST SUMMARY

Date	Test No.	Duration	Defined by	Conditions and Remarks
2-9-71	1-001	0 sec.	TD-185-001 & TCR #1	1/4" step, 1/2 lb/sec GN_2 flowrate. Engine valves did not open dur to procedure error. Repeated as 001A.
2-9-71	1-001A	3 sec.	TD-185-001 & TCR #1	1/4" step, high GN_2 flowrate. Nominal LM ullage pressures (183 psia) gave above-nominal EXNOZ engine pressures and flowrates.
2-11-71	2-004	15 sec.	TD-185-001 & TCR #2	1/4" step, high GN_2 flow. First firing with new target tank pressures to give nominal engine operation. Fuel pressure OK at 169 psia, oxidizer tank pressure dropped 13 psi during run. GN_2 manifold pressure rose 50% during firing.
2-11-71	2-004A	15 sec.	TD-185-001 & TCR's #2 and 3	Repeat of 2-004 above, with same results. After test, replaced oxidizer regulators, installed gas flowmeter and P-T sensors in GN_2 system, made GN_2 flowrate vs. manifold pressure checkout.
2-19-71	2-004B	15 sec.	TD-185-001 & TCR #3	Repeat of 2-004: 1/4" step, high GN_2 flow. Procedure error stopped tank pressurization at +5 seconds, ran in blowdown until shutdown.

Table II
Sheet 2 of 4

Extendable Nozzle Engine Test Summary (cont.)

Date	Test No.	Duration	Defined by	Conditions and Remarks
2-19-71	2-004C	15 sec	TD-185-001 & TCR #3	Repeat of 2-004B above. Oxidizer tank pressure still dropped. GN_2 manifold pressure rose 50% as before, but GN_2 flowmeter showed constant rate. Pressure rise apparently thermal effect.
2-19-71	2-003	15 sec	TD-185-001 & TCR #3	1/4" step, intermediate 0.3 lb/sec GN_2 flow.
2-19-71	2-002	15 sec	TD-185-001 & TCR #3	1/4" step, low 0.1 lb/sec GN_2 flowrate. Coolant flowrate too low (0.067 lb/sec)
2-19-71	2-002A	15 sec	TD-185-001 & TCR #3	Repeat of 2-002 above.
2-19-71	2-001	15 sec	TD-185-001 & TCR #3	1/4" step, uncooled. After test performed in-place calibration on thermocouples and calorimeters. Installed zero step height ring.
3-3-71	1-002	20 sec	TD-185-001	Zero step, uncooled baseline test.
3-4-71	1-002A	20 sec	TD-185-001	Repeat of . 002 above for data repeatibility. Installed 1/2" step ring after test.
3-9-71	3-004	30 sec	TD-185-001 & TCR #4	1/2" step, high (0.5 lb/sec) GN_2 flow. Had to cycle oxidizer pressurization valve to prevent tank overpressurization.

Extendable NozzleEngine Test Summary (cont.)

Date	Test No.	Duration	Defined by	Conditions and Remarks
3-9-71	3-003	30 sec	TD-185-001 & TCR #4	1/2" step, 0.3 lb/sec GN_2 flowrate.
3-9-71	3-002	30 sec.	TD-185-001 & TCR #4	1/2" step, 0.1 lb/sec GN_2 flowrate.
3-9-71	3-001	30 sec	TD-185-001 & TCR #4	1/2" step, uncooled. Installed 3/4" step and boundary layer temperature probes after test.
3-25-71	4-004	30 sec	TD-185-001 & TCR #5	3/4" step, 0.5 lb/sec GN_2 flow.
3-25-71	4-003	30 sec	TD-185-001 & TCR #5	3/4" step, 0.3 lb/sec GN_2 flow.
3-25-71	4-002	30 sec	TD-185-001 & TCR #5	3/4" step, 0.1 lb/sec GN_2 flowrate.
3-25-71	4-001	30 sec	TD-185-001 & TCR #6	3/4" step, uncooled. Measured throat (19.09 $in.^2$) and replaced actuators.
4-2-71	5-001	30 sec	TD-185-001 & TCR #6	1/2" step, extendable skirt retracted 2 inches throughout firing, high GN_2 coolant flow. Cycled oxidizer pressure valve to prevent overpressurization.
4-2-71	5-002	30 sec	TD-185-001 & TCR #6	1/2" step, skirt retracted 2 inches, low 0.1 lb/sec GN_2 flow.
4-2-71	5-003	30 sec	TD-185-001 & TCR #6	1/2" step, skirt retracted 2 inches, uncooled.

Extendable Nozzle Engine Test Summary (cont.)

Date	Test No.	Duration	Defined by	Conditions and Remarks
4-6-71	5-004	17 sec	TD-185-001 & TCR #6	1/2" step, 0.5 lb/sec GN_2, moving nozzle. Skirt retracted satisfactorily but only extended halfway until shutdown. After test increased actuation pressure, re-routed hydraulic vent lines, valves unpowered between actuations.
4-14-71	5-004A	38 sec	TD-185-001 & TCR #7	1/2" step, retracted and extended nozzle twice during firing, once with high GN_2 coolant flow, once uncooled.

TOTAL DURATION 548

Table II
Sheet 4 of 4

TABLE III

THERMAL INSTRUMENTATION SUMMARY

Axial Distance, Inch	Chamber Dia. in.	Area Ratio	Thermocouple Number	Thermocouple Angle	Calorimeter Number	Calorimeter Angle	Gas Probe Number	Gas Probe Angle
1.567	22.375	Step Region	1	6	1	0		
			2	126				
			3	246				
2.097	22.375	Step Region	4	18	2	120	2	120
			5	138	3	240		
			6	258				
2.447	22.375	Step Region	7	6	4	132	3	
			8	126	5	252		
			9	246				
2.787	22.375	Step Region	10	18	6	0		
			11	138				
			12	258				
3.417	22.68	21.1	13	6	7	12	4	120
			14	126	8	120		
			15	246	9	240		
4.167	23.24	22.3	16	18				
			17	138				
			18	258				
9.267	26.52	28.9	19	6				
			20	126				
			21	246				
13.167	28.76	33.9	22	6				
			23	126				
			24	246				

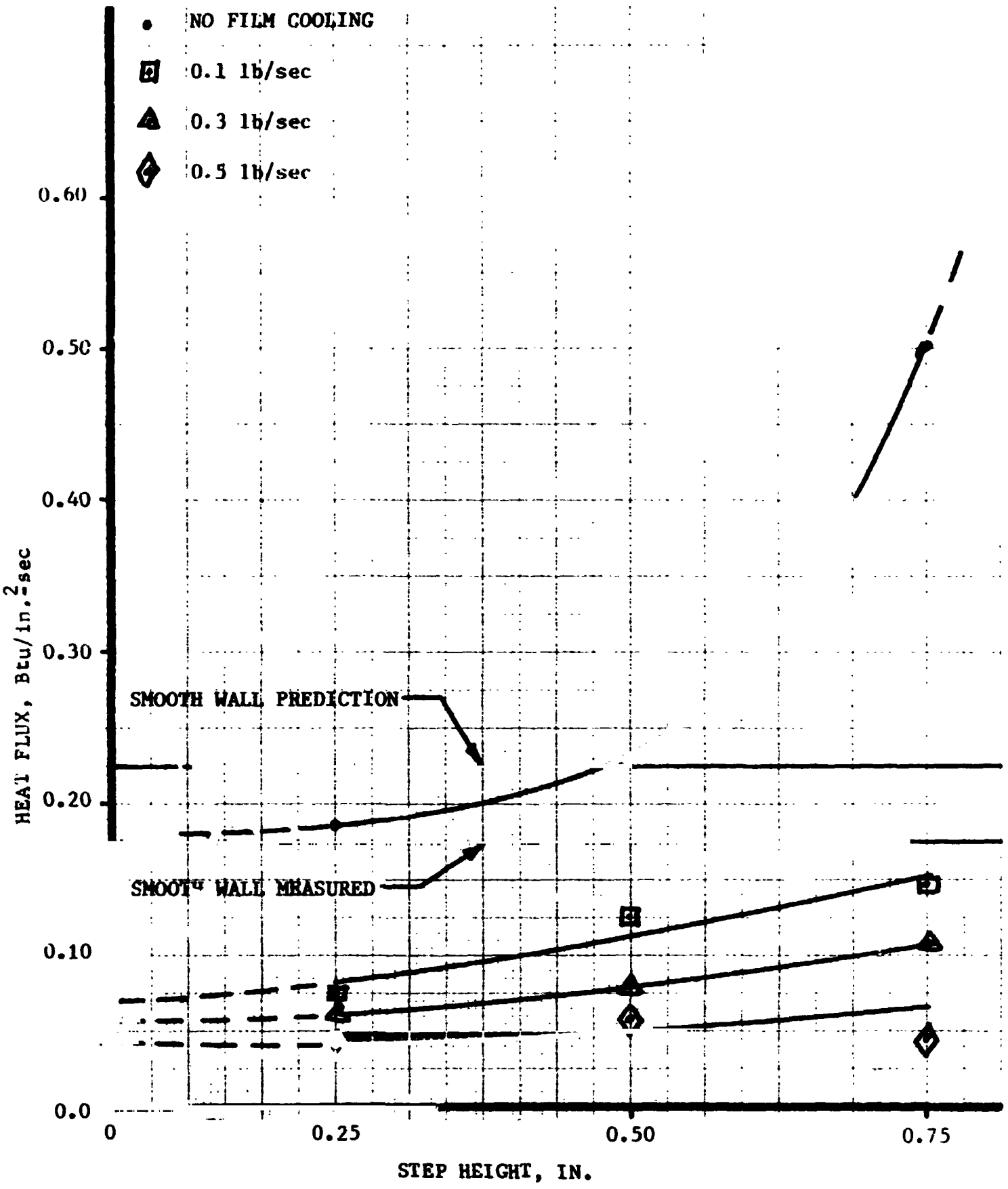

Heat Flux vs Step Height

Figure 1

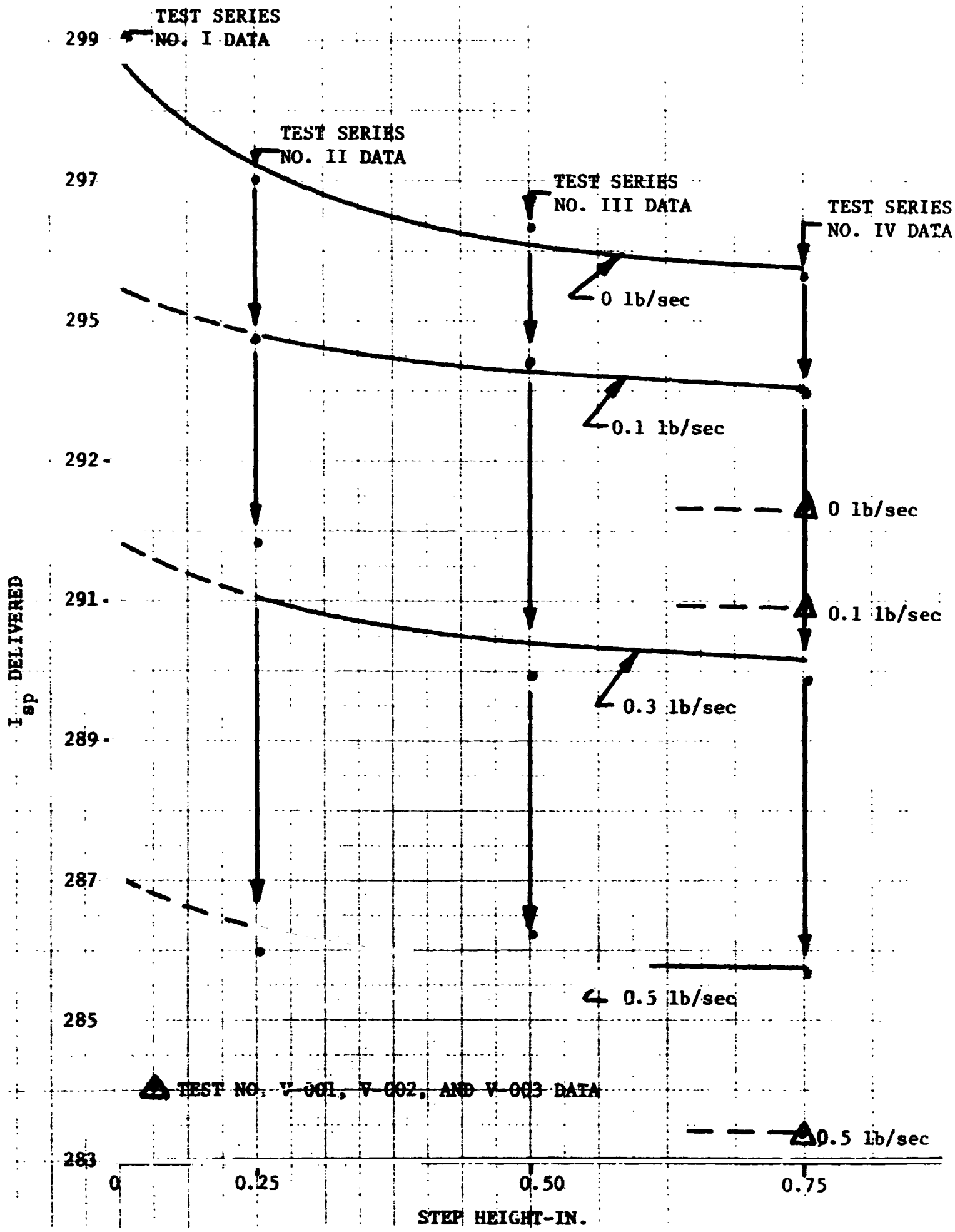

Delivered I_{sp} vs Step Height

Figure 2

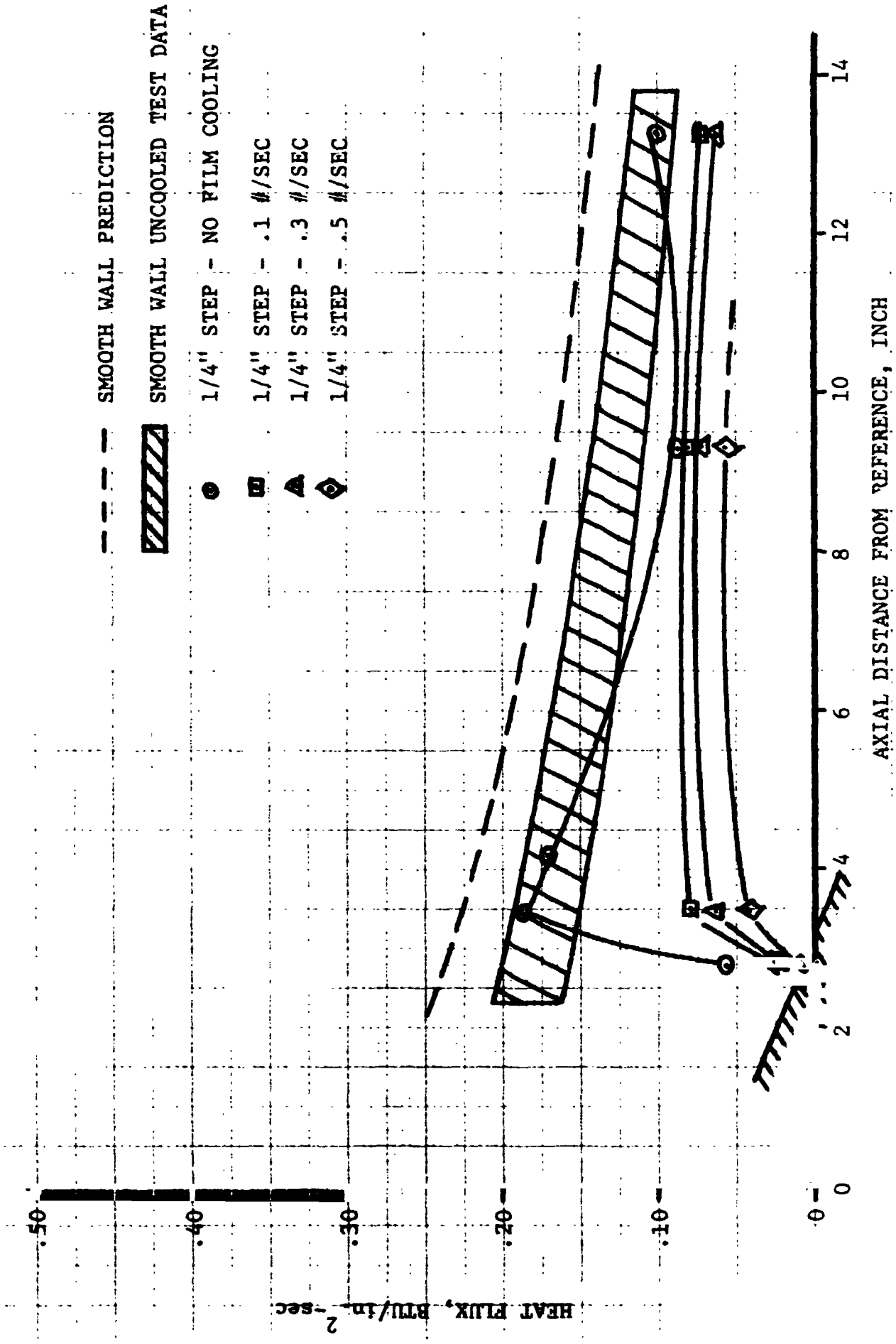
SMOOTH WALL PREDICTION
SMOOTH WALL UNCOOLED TEST DATA
1/4" STEP - NO FILM COOLING
1/4" STEP - .1 #/SEC
1/4" STEP - .3 #/SEC
1/4" STEP - .5 #/SEC
HEAT FLUX, BTU/in.2-sec
.50
.40
.30
.20
.10
0
0
2
4
6
8
10
12
14
AXIAL DISTANCE FROM REFERENCE, INCH
Test Series II Heat Flux Data: 0.25-in. Step

Figure 3

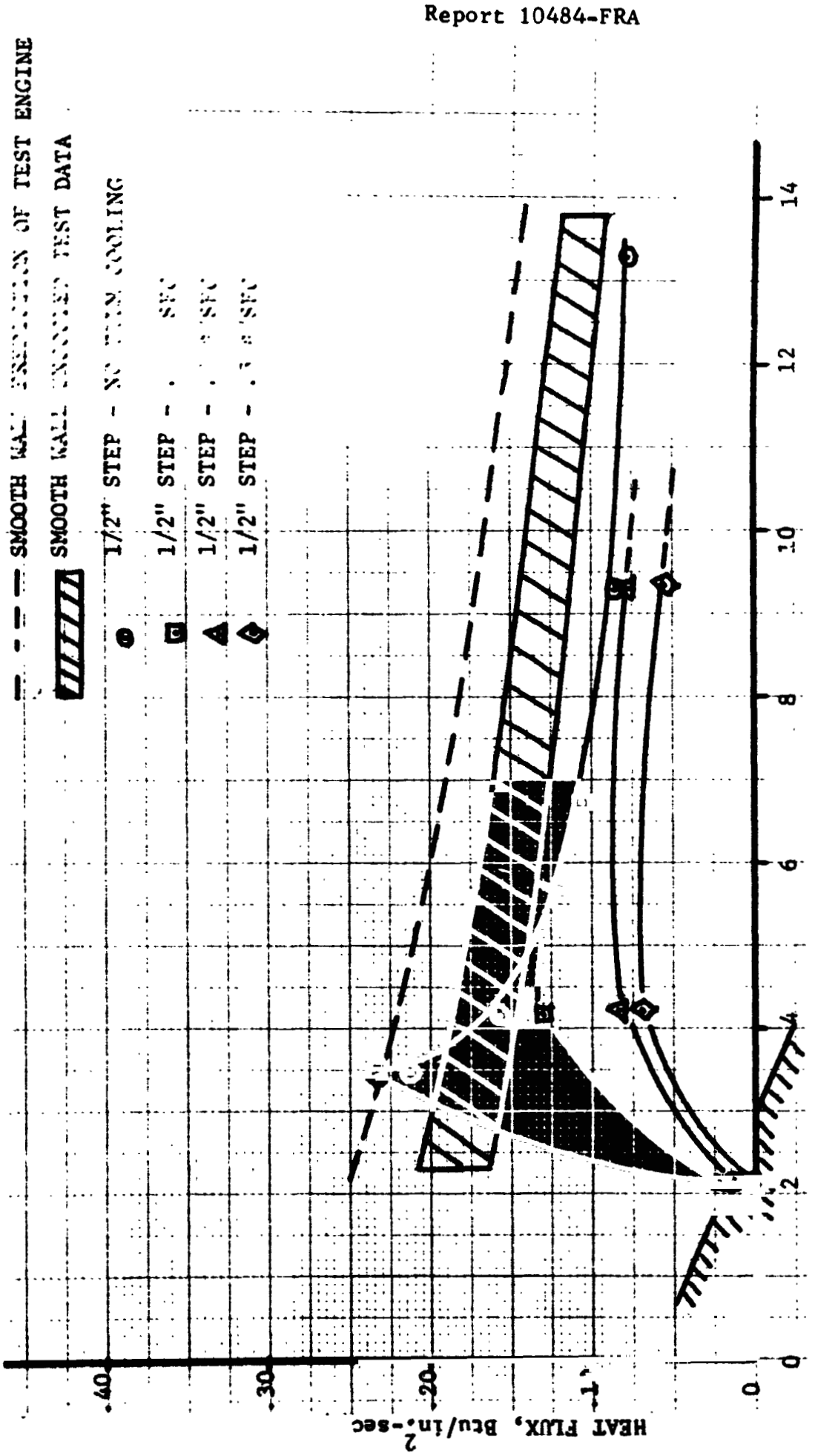

Test Series III Heat Flux Data: 0.50-in. Step

Figure 4

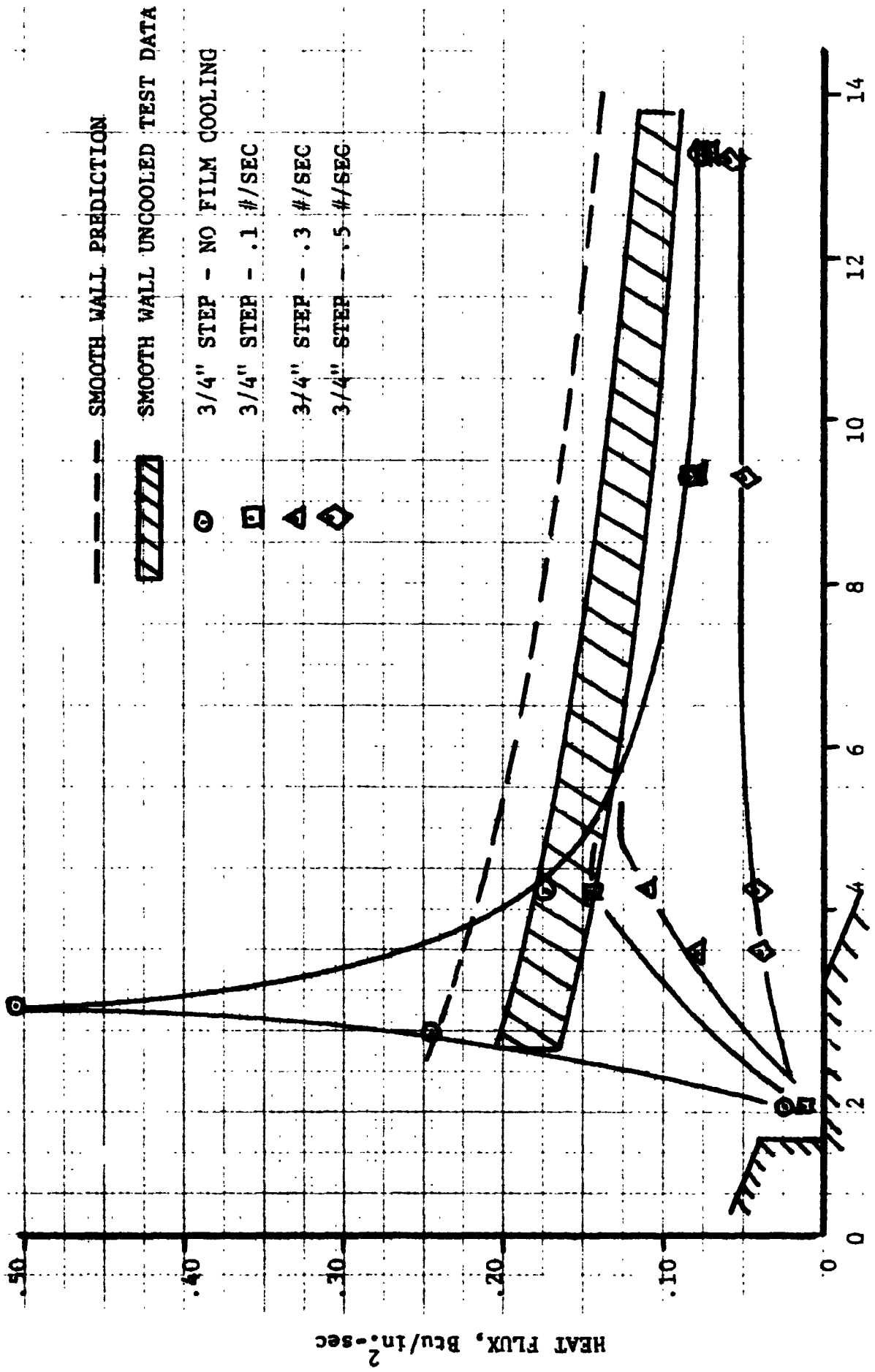
SMOOTH WALL PREDICTION
SMOOTH WALL UNCOOLED TEST DATA
3/4" STEP - NO FILM COOLING
3/4" STEP - .1 #/SEC
3/4" STEP - .3 #/SEC
3/4" STEP - .5 #/SEC
HEAT FLUX, Btu/in.²-sec
.50
.40
.30
.20
.10
0
2
4
6
8
10
12
14
AXIAL DISTANCE FROM REFERENCE, in.
Test Series IV Heat Flux Data: 0.75-in. Step

Figure 5

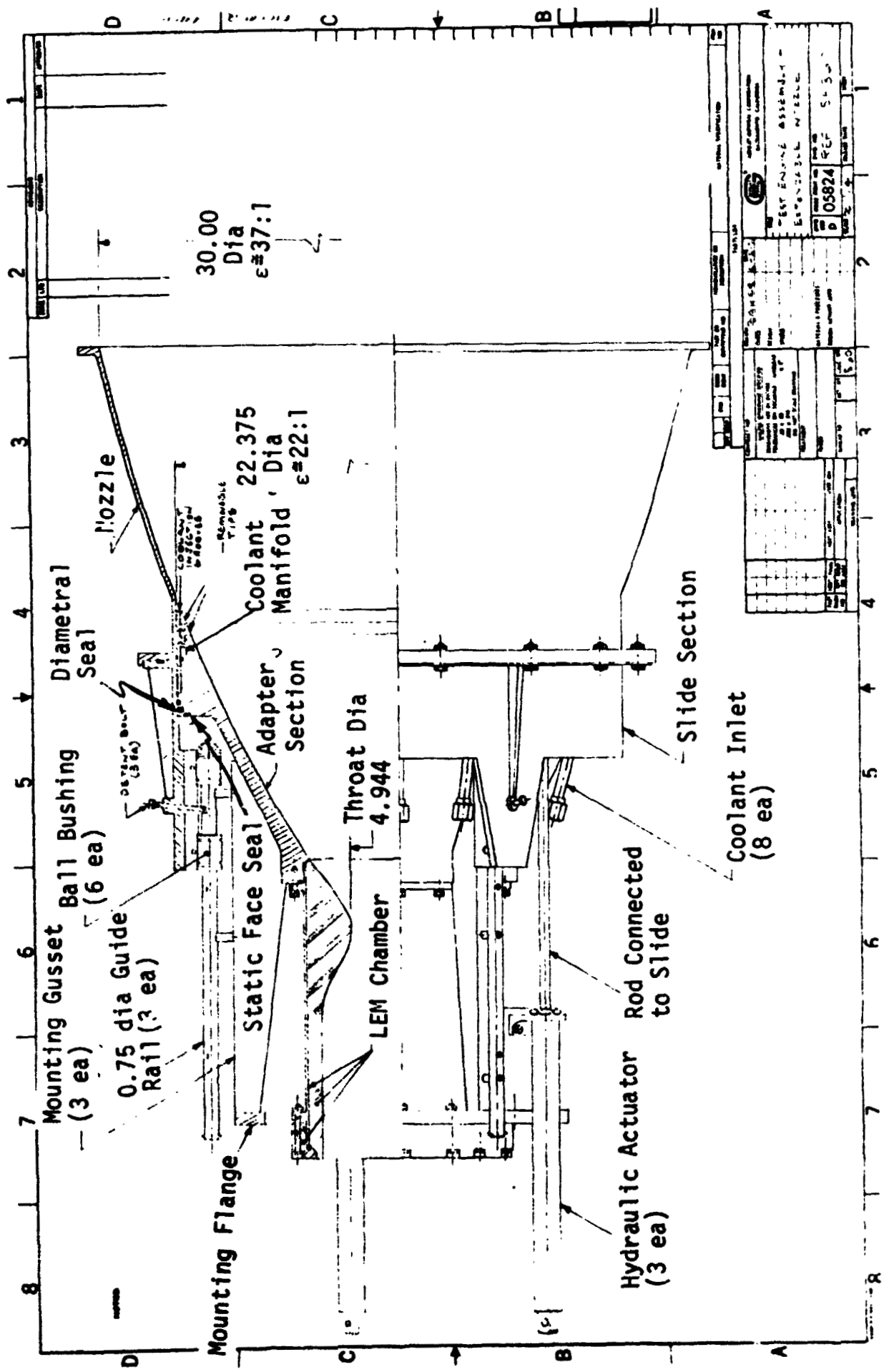

Figure 6

Extendable Nozzle Test Engine Assembly

Design Guide Prediction with 3.0 Amplification Factor

Design Guide Prediction with 1.0 Amplification Factor

Smooth Wall Prediction

Series III, Test -003 Data (0.5-in. Step, 0.318 lb/sec GN_2 Film Cooling)

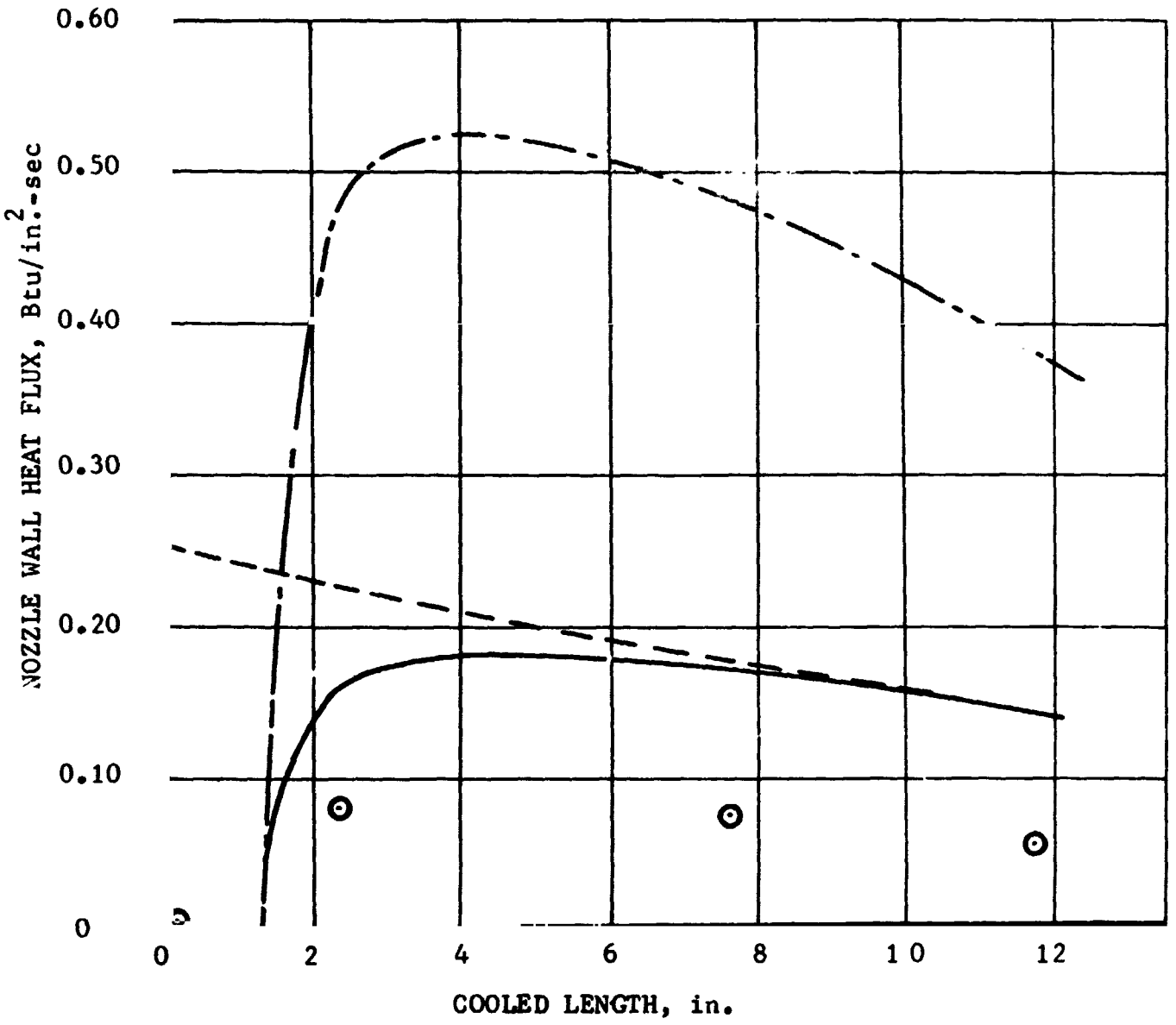

Nozzle Wall Heat Flux with Film Cooling

Figure 7

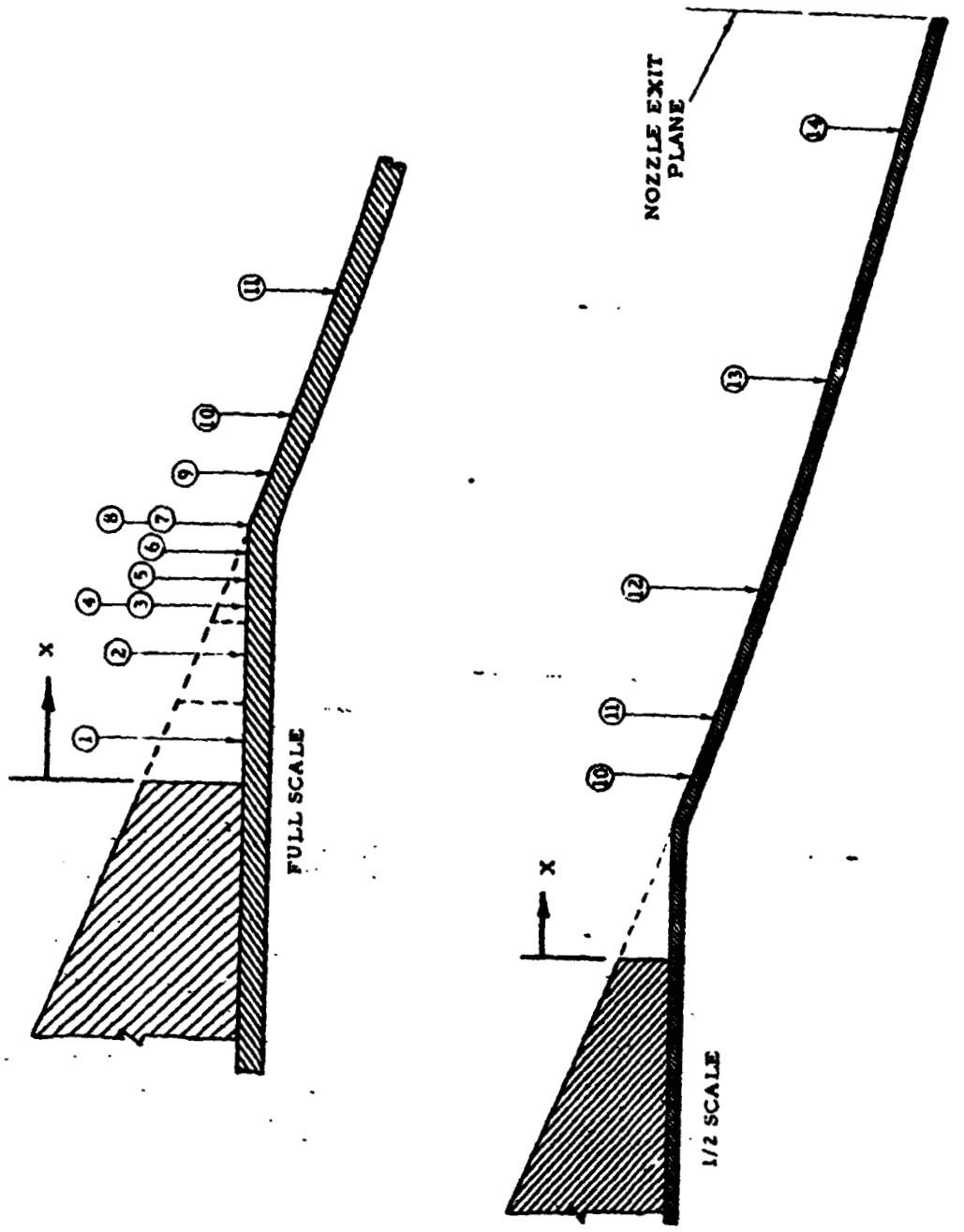

PRESSURE TAP NO.	X INCHES
1	.35
2	1.00
3	1.38*
4	1.38
5	1.58
6	1.79
7	2.00*
8	2.00
9	2.39
10	2.85
11	3.80
12	5.75
13	9.00
14	12.90

* NOTE: All pressure taps are in line with coolant passages except PT #3 and #7.

Nozzle Wall Pressure Taps for Test Engine

Figure 8

T = Thermocouple (24 ea)
C = Calorimeter (9 ea)
P = Pressure Transducer (14 ea)

INSTRUMENTATION	AT STATION
P1	A
C1, T1, T2, T3	B
C2, C3, T4, T5, T6	C
P2	D
C4, C5, T7, T8, T9	E
P3, P4	F
P5	G
C6, T11, T12	H
P6	J
P7, P8	K
C7, C8, C9, T13, T14, T15	L
P9	M
P10	N
T16, T17, T18	O
P11	P
P12	Q
T19, T20, T21	R
P13	S
T22, T23, T24	T
P14	U

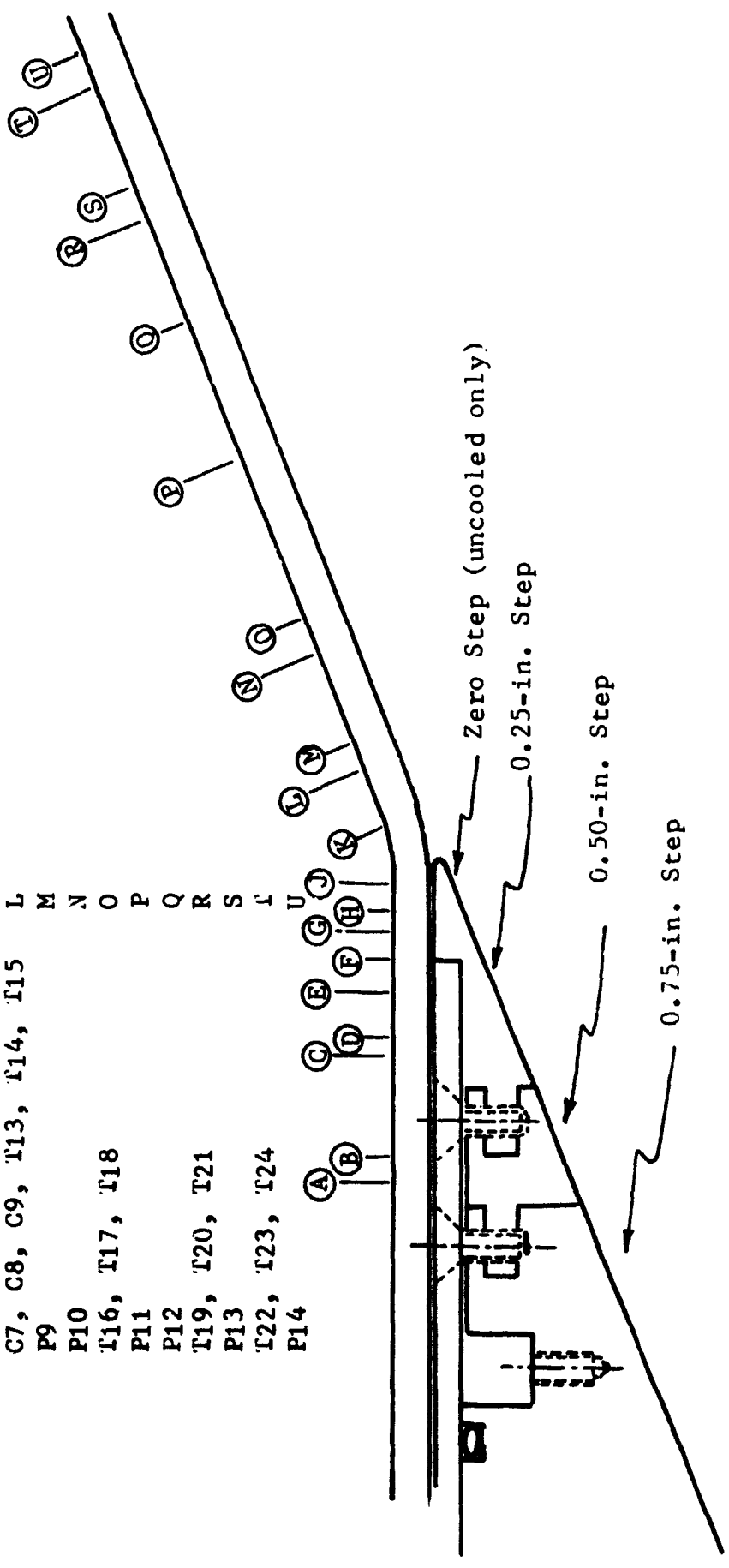

Instrumentation in Region of Removable Tips

Figure 9

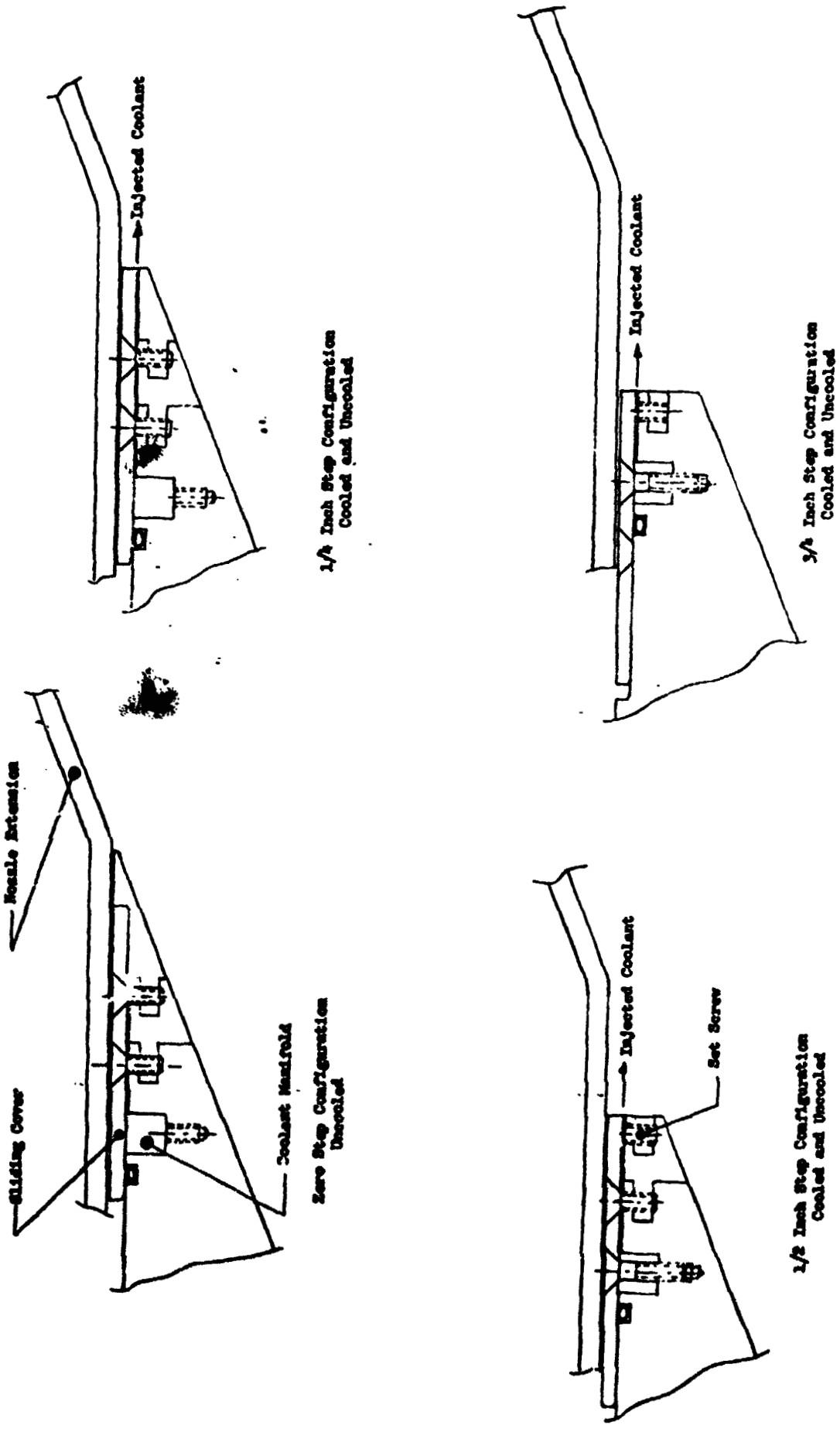

Variable Step Removable Tip Concept

Figure 10

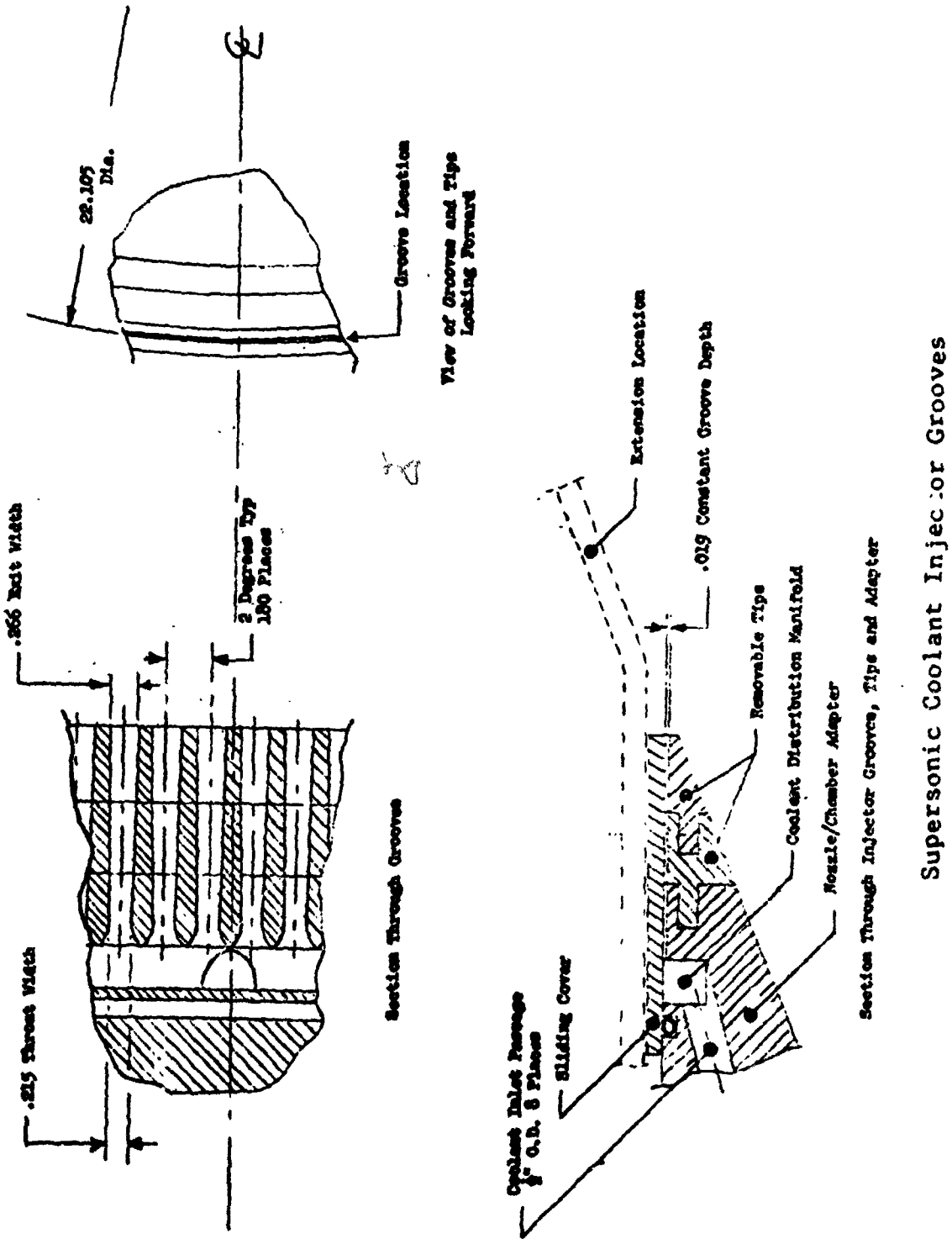

Supersonic Coolant Injector Grooves

Figure 11

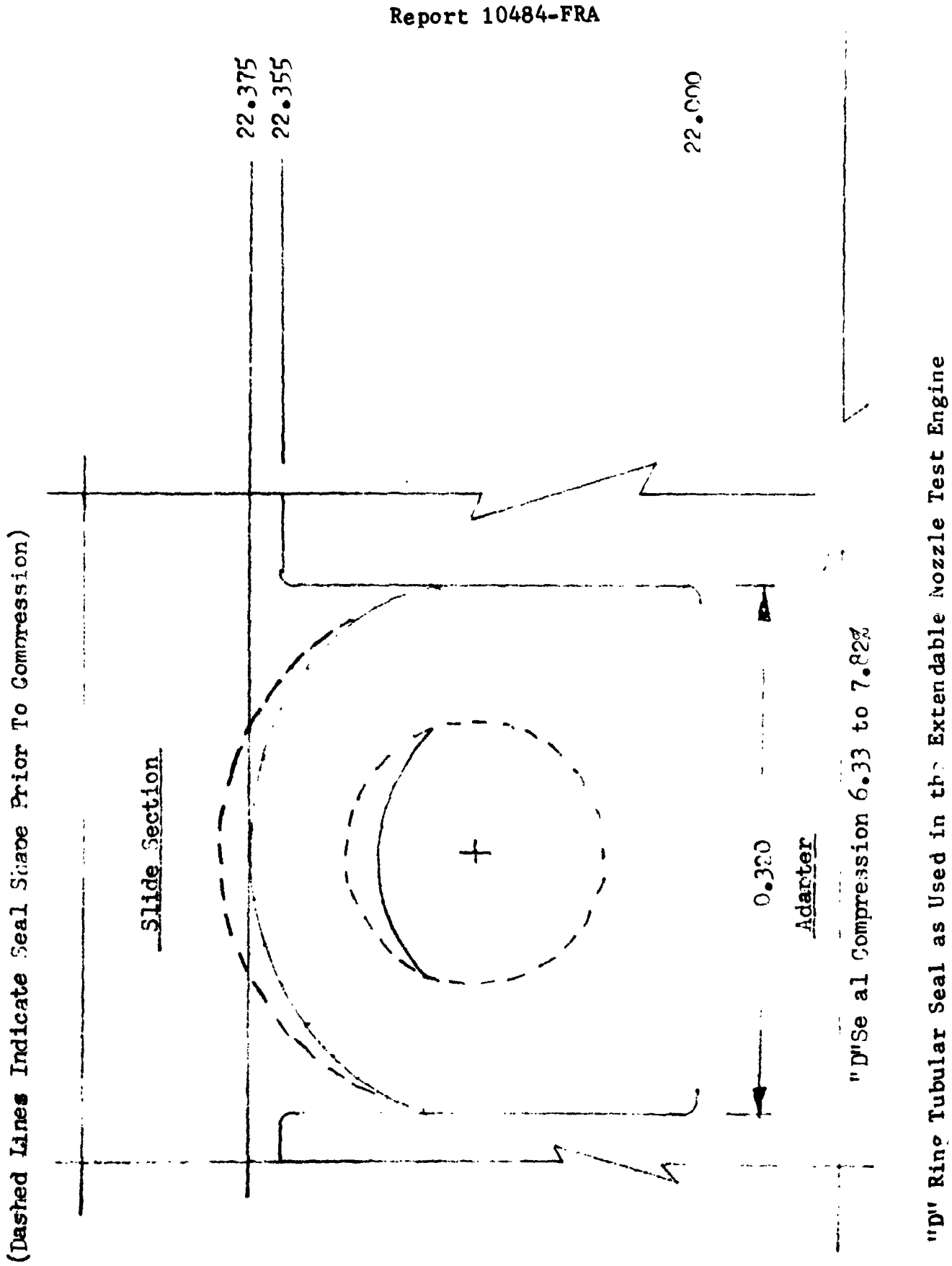
22.375
22.355
22.000
Slide Section
0.320
Adapter
(Dashed Lines Indicate Seal Shape Prior To Com
"D"Se al Compression 6.33 to 7.82
"D" Ring Tubular Seal as Used in th Extenda
Test Engine

Figure 12

Engine Installed in Stand, Showing Pressure Instrumentation

Figure 13

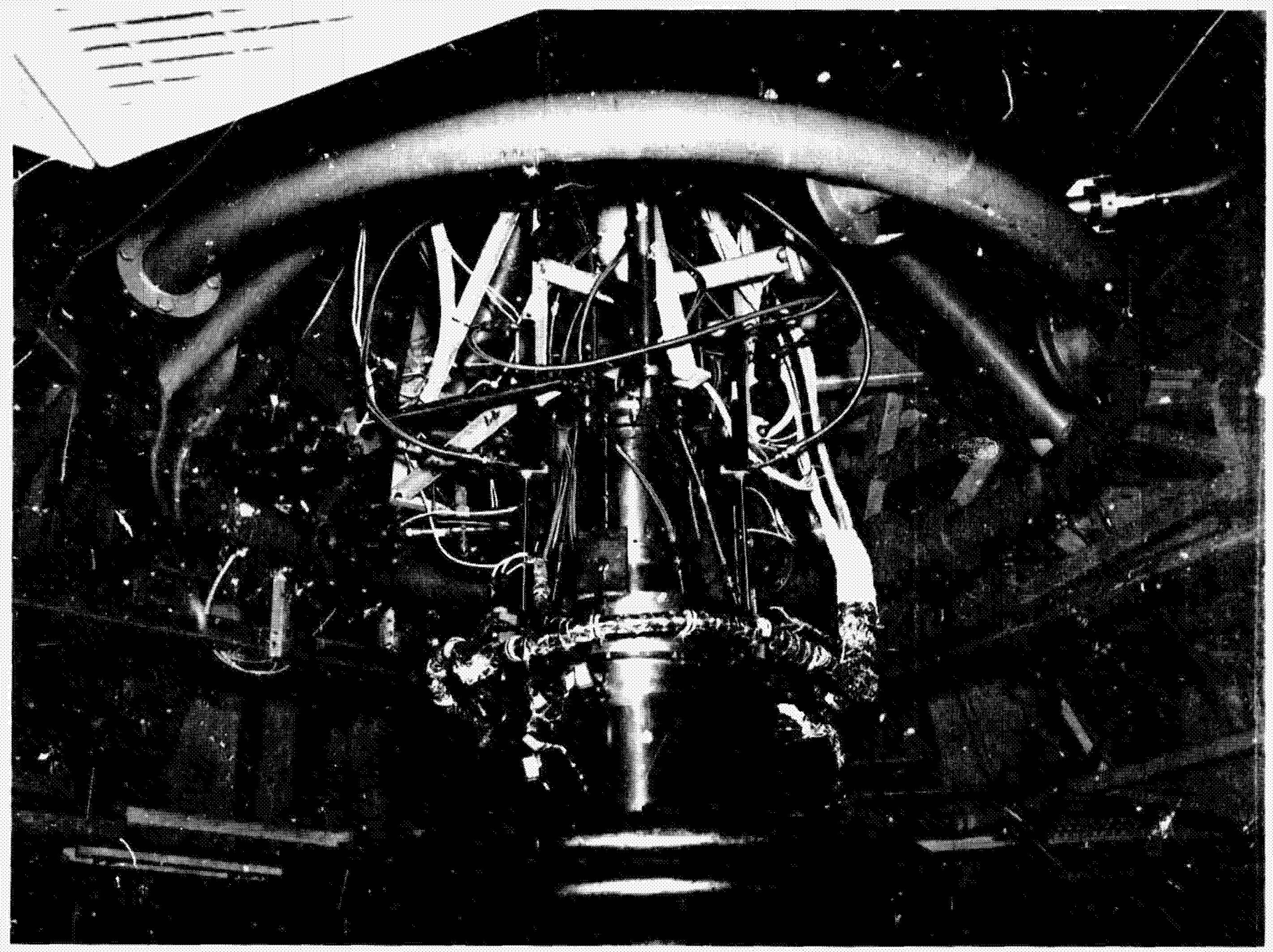

Figure 14

Engine Installed in Stand, Showing Thermal Instrumentation

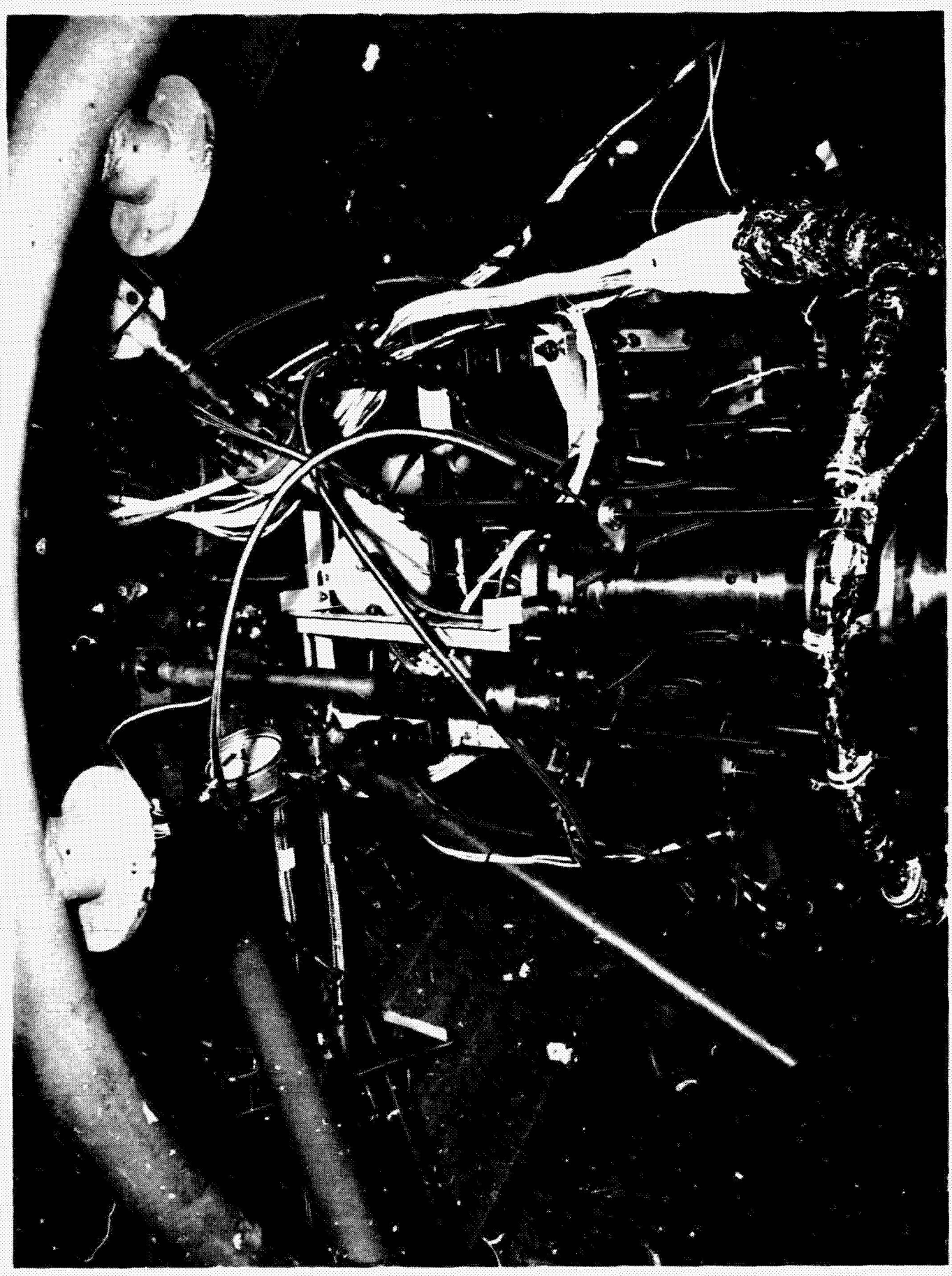

Engine Installed in Stand, Showing LEM Ascent Portion

Figure 15

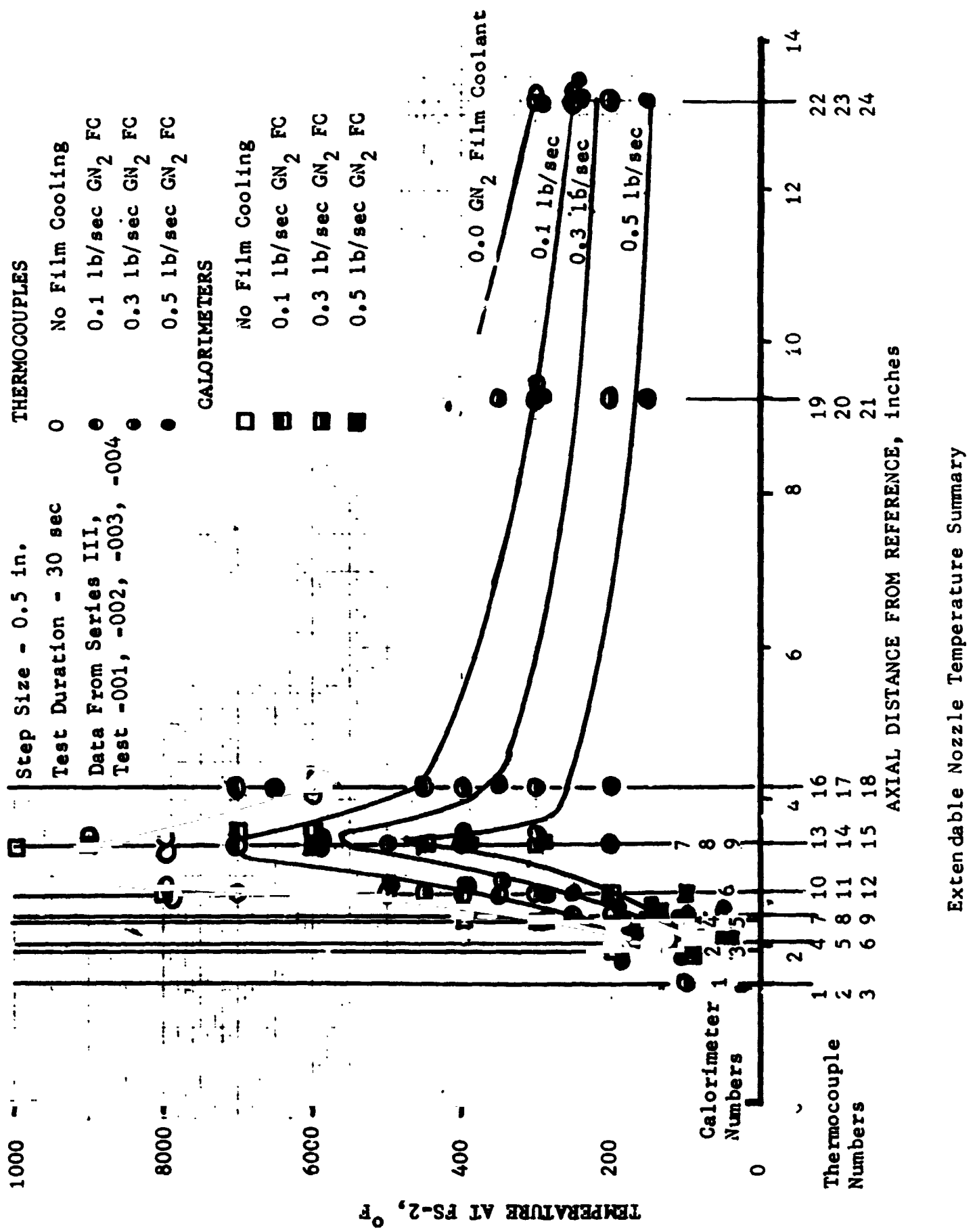
THERMOCOUPLES
No Film Cooling
0.1 lb/sec GN2 FC
0.3 lb/sec GN2 FC
0.5 lb/sec GN2 FC
CALORIMETERS
No Film Cooling
0.1 lb/sec GN2 FC
0.3 lb/sec GN2 FC
0.5 lb/sec GN2 FC
Step Size - 0.5 in.
Test Duration - 30 sec
Data From Series III,
Test -001, -002, -003, -004
0.0 GN2 Film Coolant
0.1 lb/sec
0.3 lb/sec
0.5 lb/sec
TEMPERATURE AT FS-2, °F
1000
8000
6000
400
200
0
Calorimeter Numbers
Thermocouple Numbers
AXIAL DISTANCE FROM REFERENCE, inches
Extendable Nozzle Temperature Summary

Figure 16

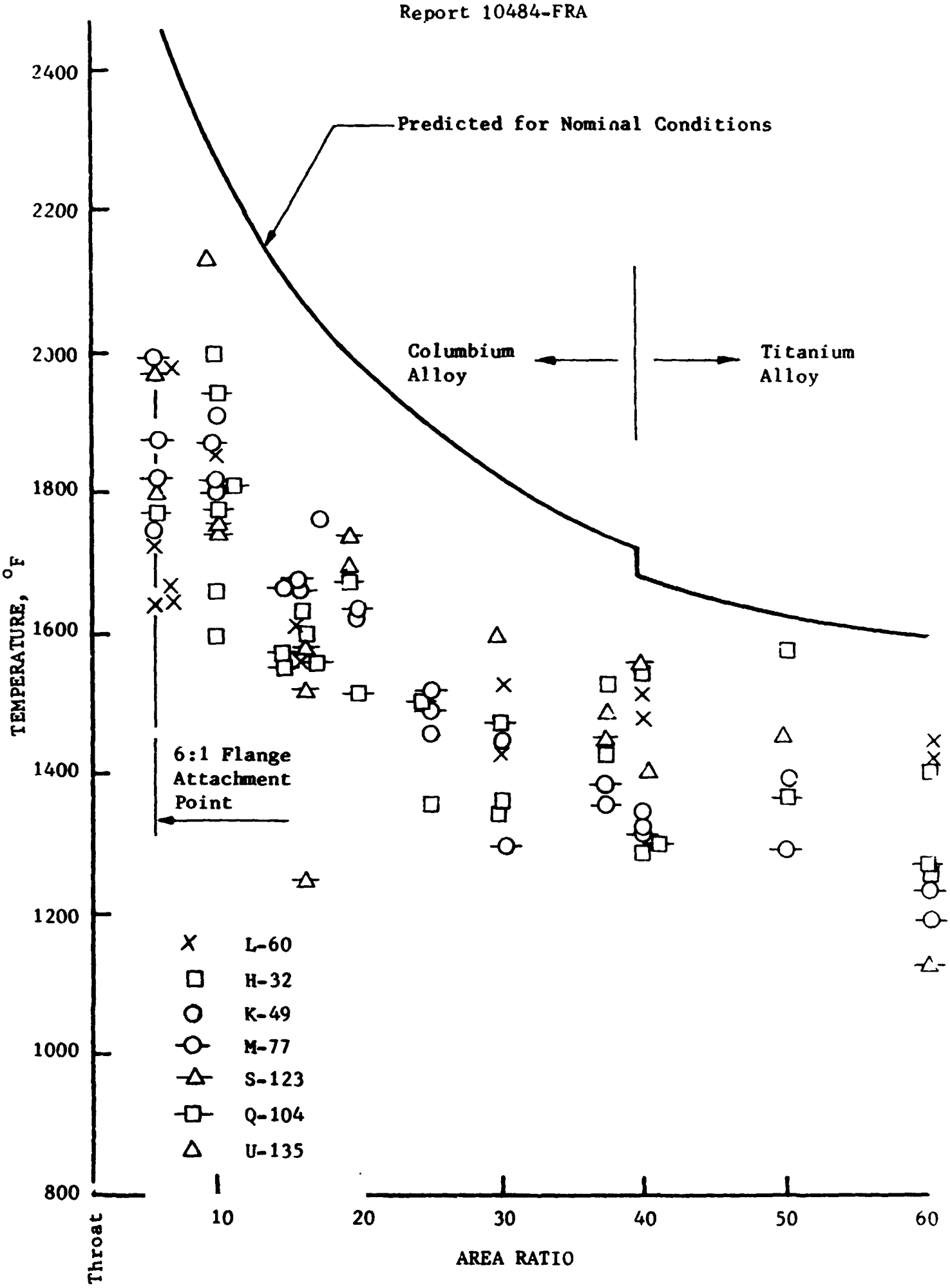

Apollo Nozzle Steady-State Temperature Data

Figure 17

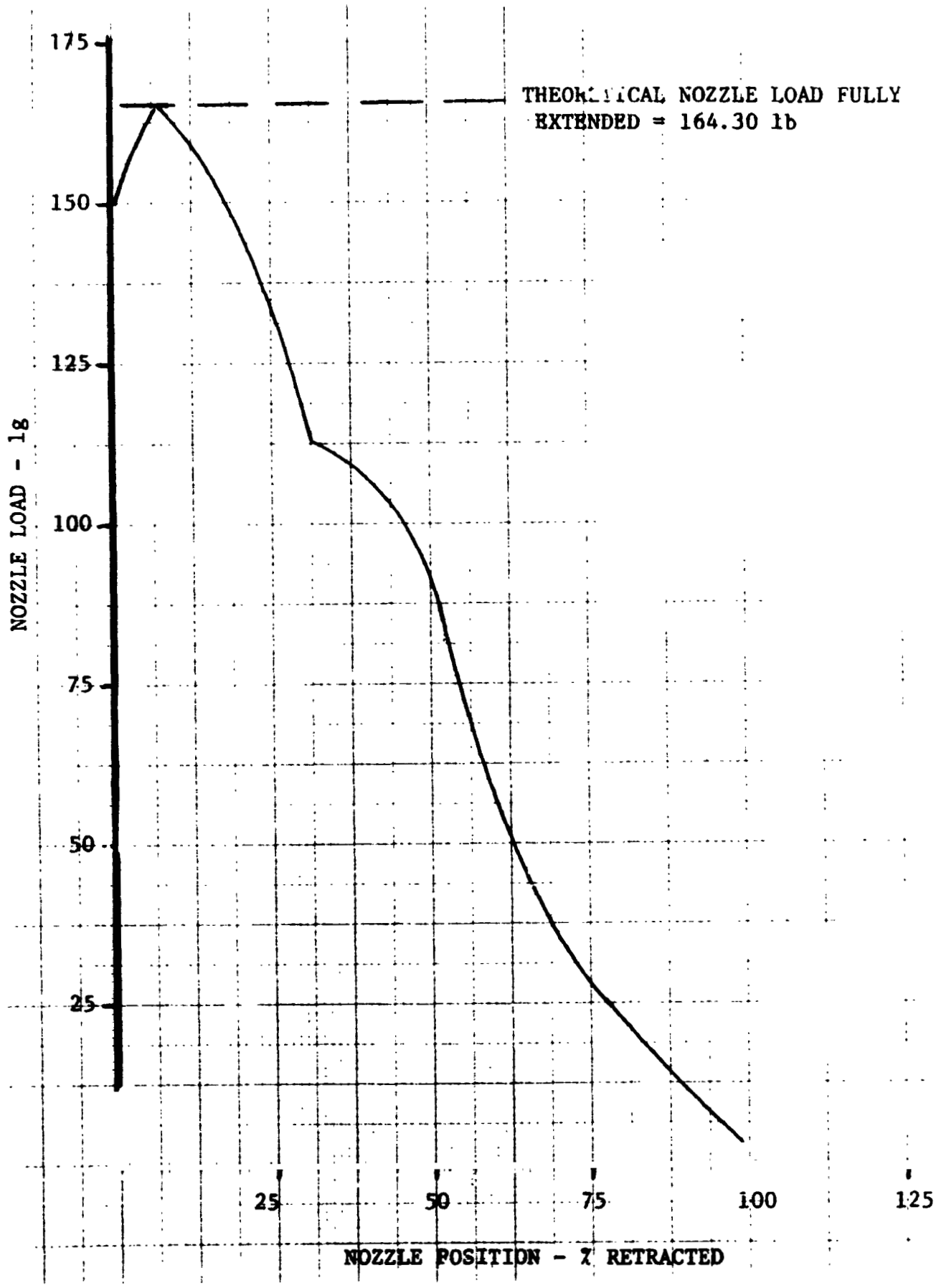

e Load vs Nozzle Position - Extend Cycle

Figure 1

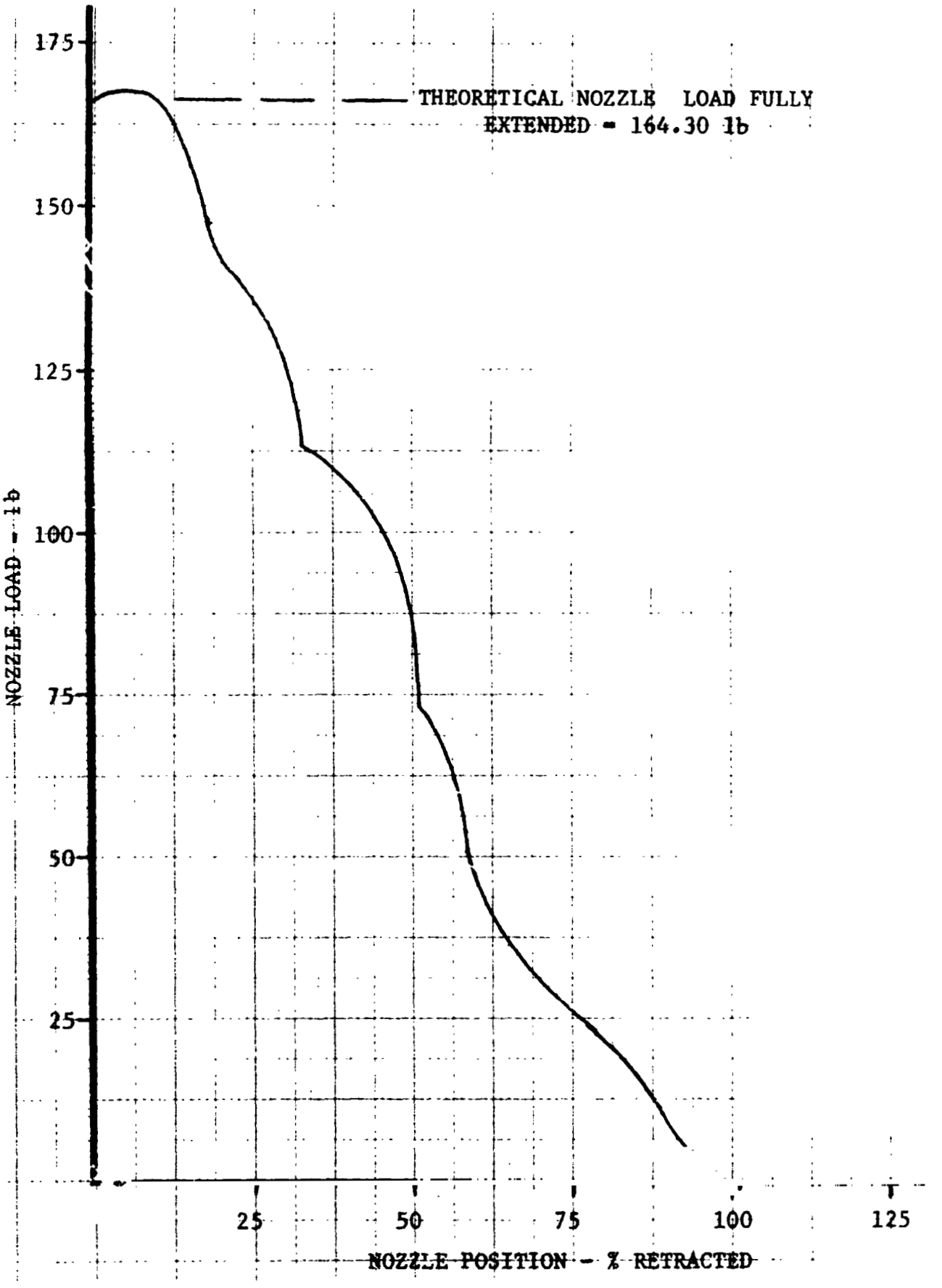

Nozzle Load vs Nozzle Position - Retract Cycle

Figure 19

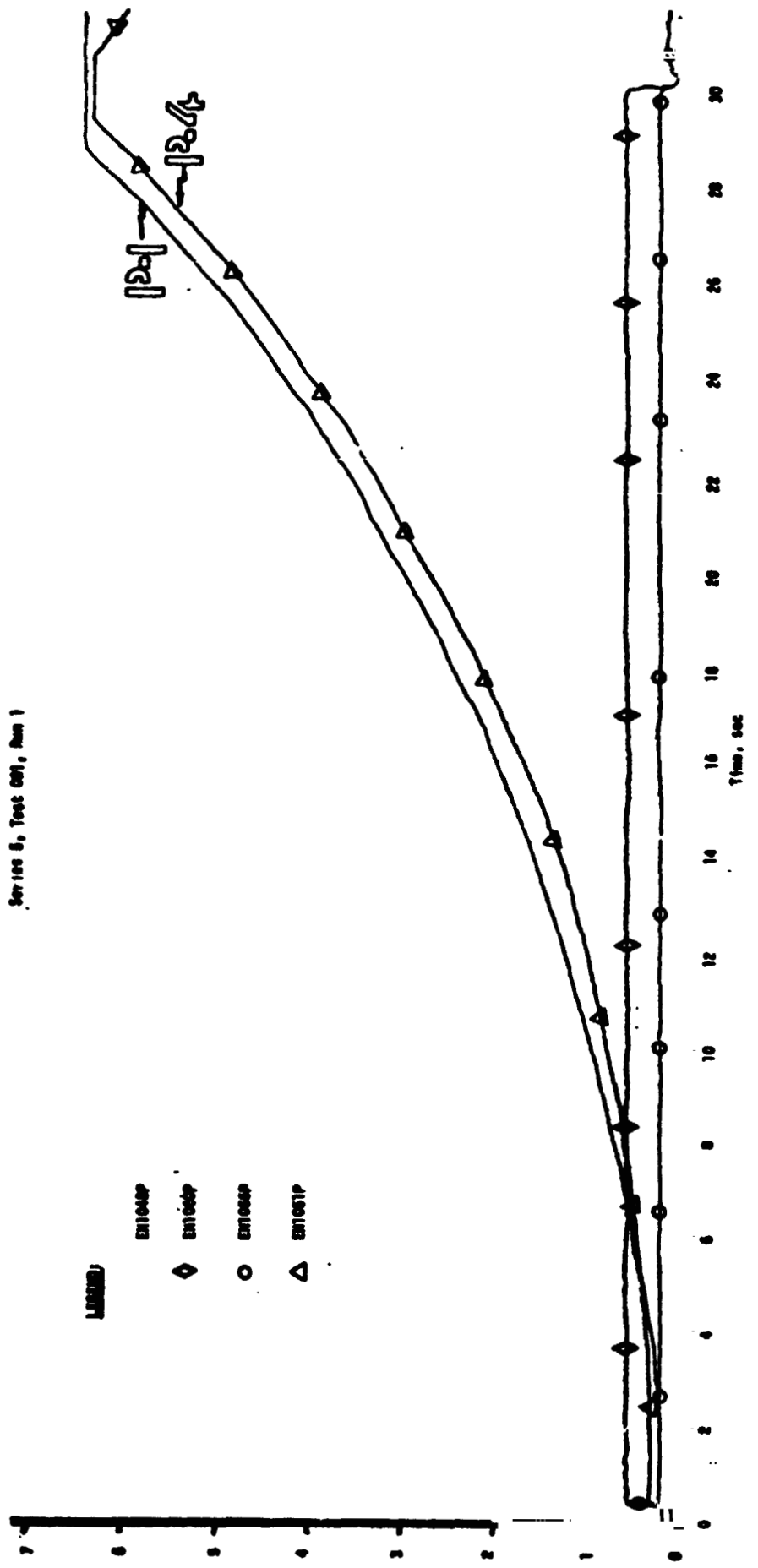

Nozzle Wall Pressures (Transducers P-1, P-4) vs Time

Figure 20

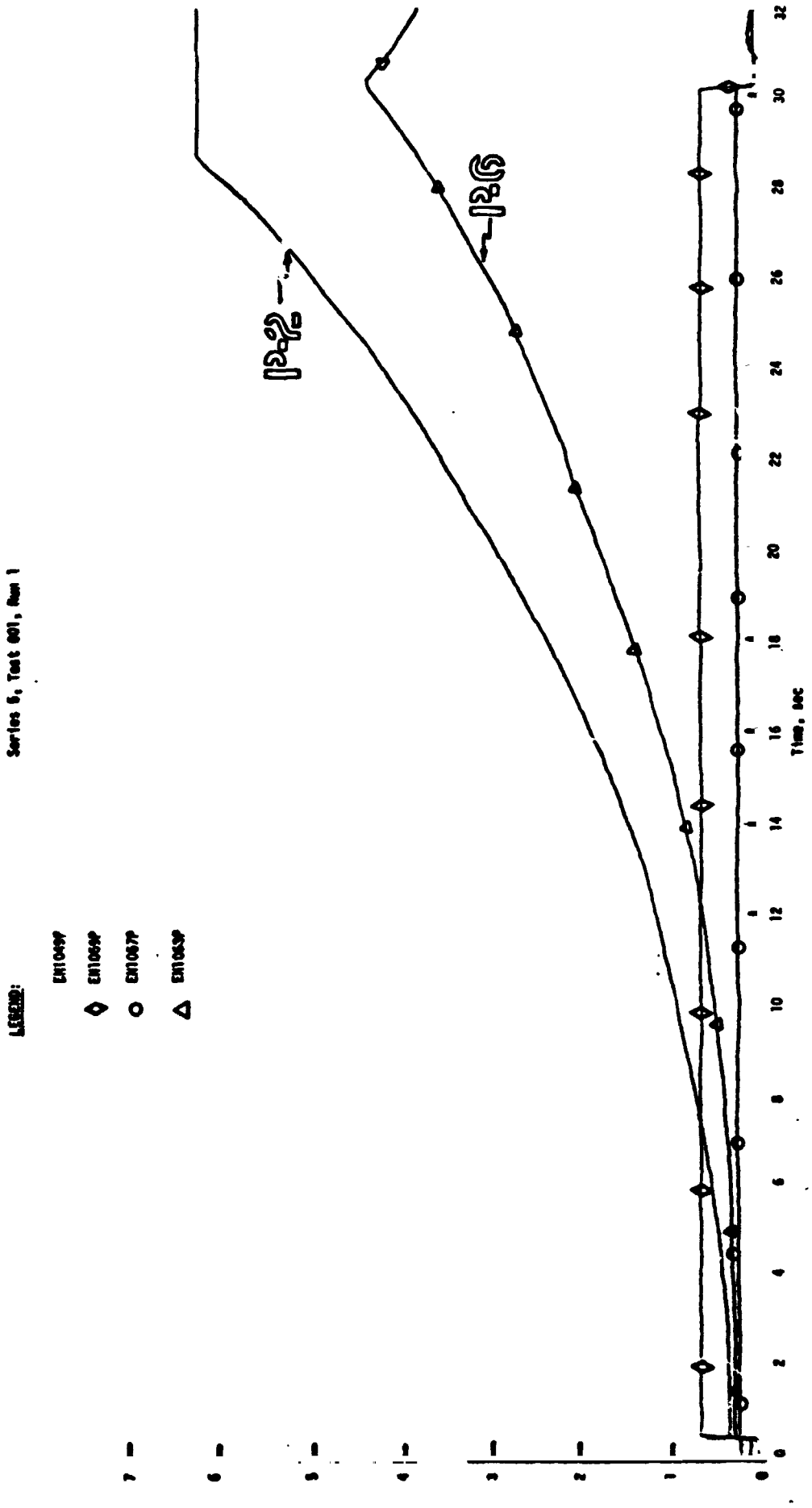

Nozzle Wall Pressures (Transducers P-2, P-6) vs Time

Figure 21

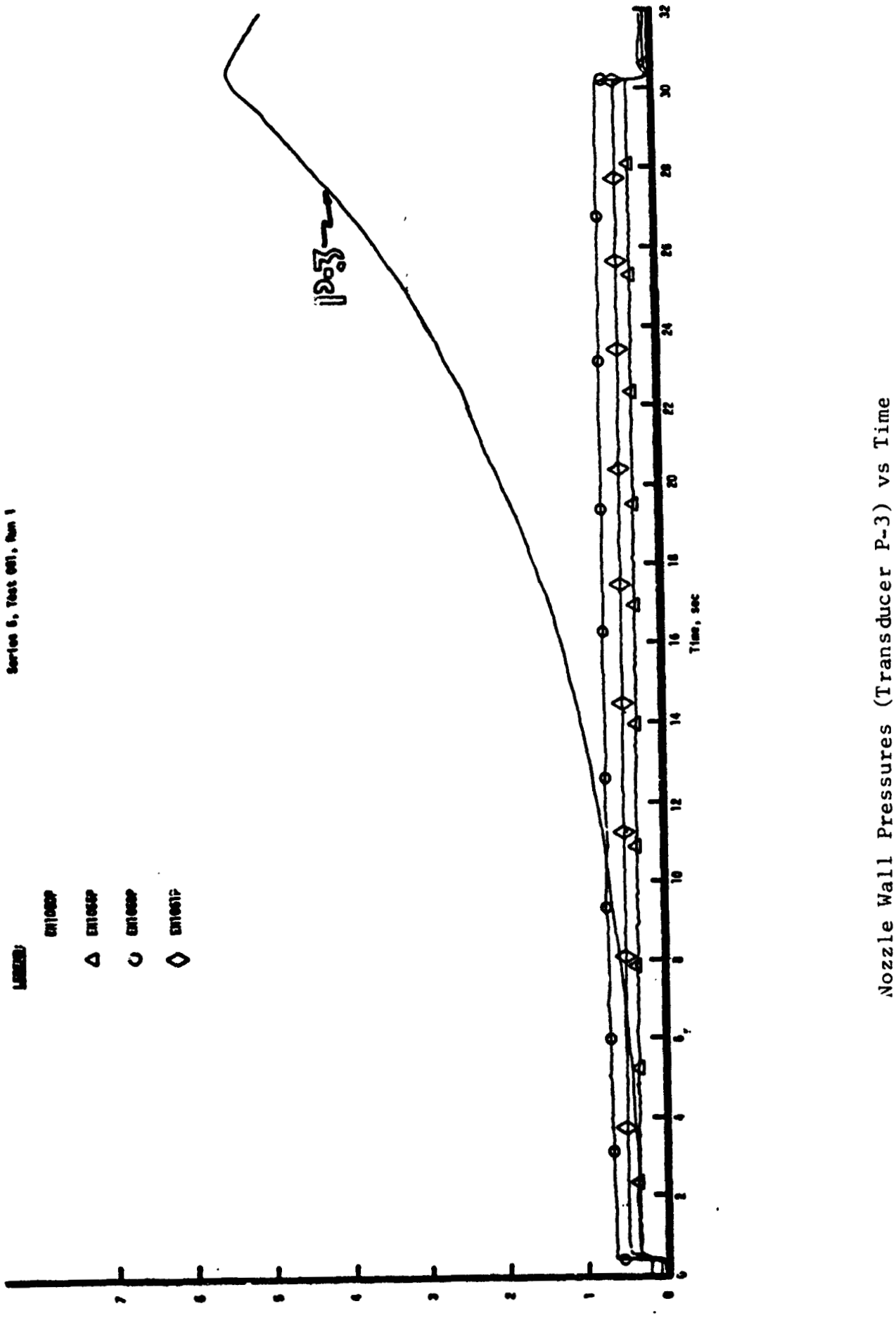

Nozzle Wall Pressures (Transducer P-3) vs Time

Figure 22

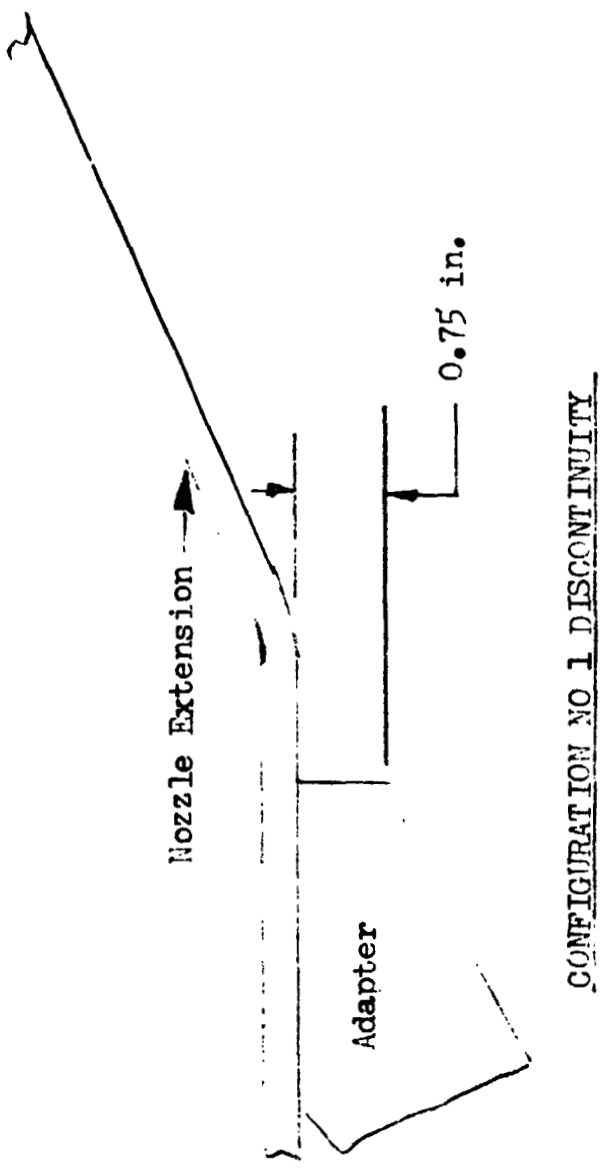

Comparison of 0.75-in. Nozzle Wall Discontinuities

Figure 23

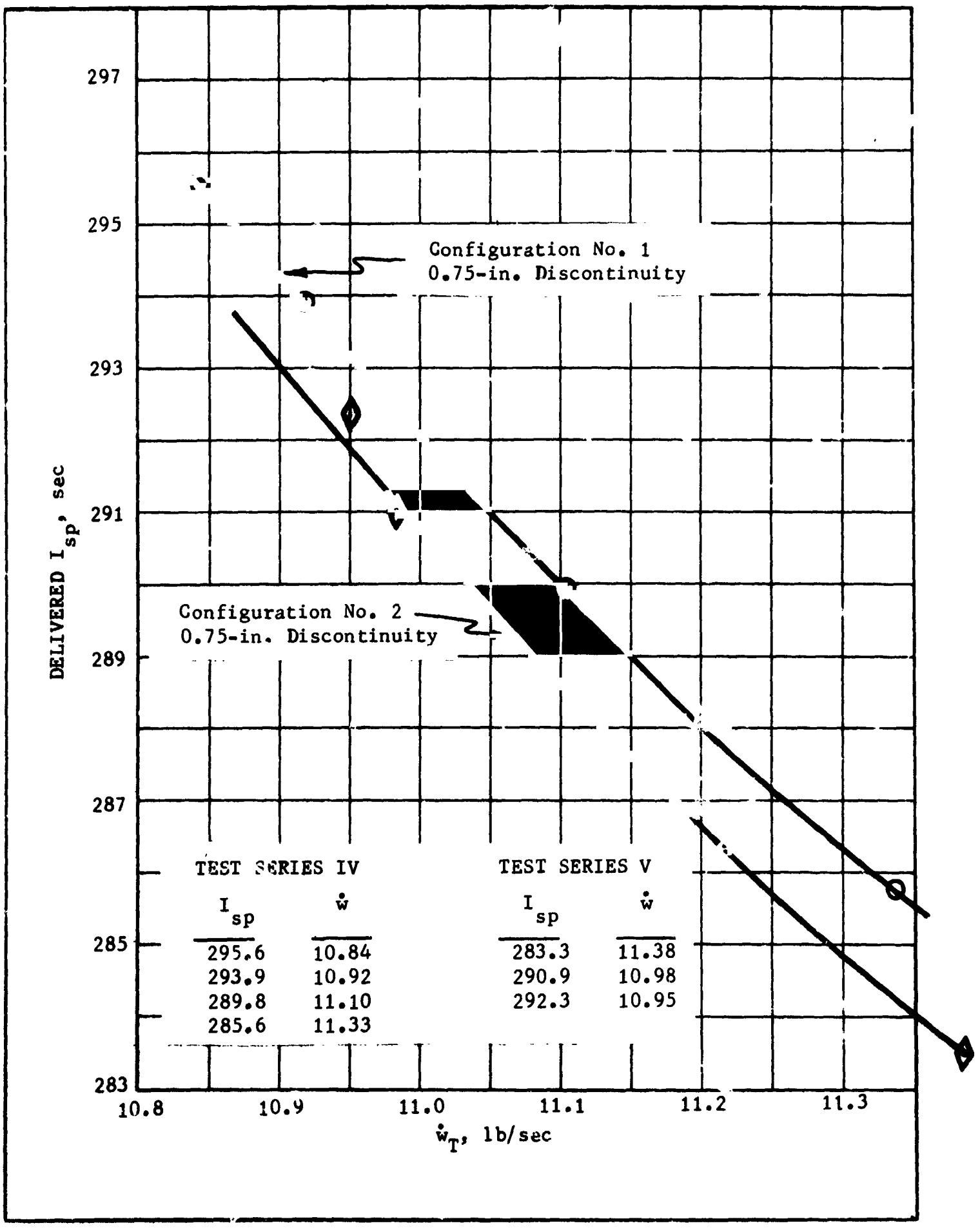

Effect of Configuration on Performance (0.75-in. Step)

Figure 24